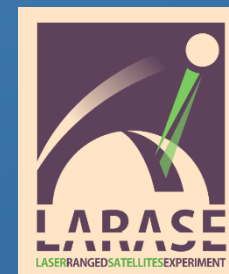




Testing General Relativity with Satellite Laser Ranging and the LAser RAnged Satellites Experiment (LARASE) research program: current results and perspectives



David M. Lucchesi(1,2,3), L. Anselmo(3), M. Bassan (2,4), C. Magnafico(1,2), C. Pardini(3),
R. Peron(1,2), G. Pucacco(2,4), R. Stanga(5,6), M. Visco(1,2)

1. Istituto di Astrofisica e Planetologia Spaziali (IAPS/INAF), Via Fosso del Cavaliere n. 100, 00133 Tor Vergata – Roma, Italy
2. Istituto Nazionale di Fisica Nucleare (INFN), sezione di Roma Tor Vergata, Via della Ricerca Scientifica n. 1, 00133 Tor Vergata – Roma, Italy
3. Istituto di Scienza e Tecnologie della Informazione (ISTI/CNR), Via Moruzzi n. 1, 56124 Pisa, Italy
4. Dipartimento di Fisica, Università di Roma Tor Vergata, Via della Ricerca Scientifica n. 1, 00133 Tor Vergata – Roma, Italy
5. Dipartimento di Fisica, Università di Firenze, Via Giovanni Sansone n. 1, 50019 Firenze, Italy
6. Istituto Nazionale di Fisica Nucleare (INFN), sezione di Firenze, Via Giovanni Sansone n. 1, 50019 Firenze, Italy

Summary

- The LARASE experiment and its goals
- The internal structure of the two LAGEOS satellites
- The rotational dynamics and the Spin Model for the LAGEOS and LARES satellites
- Neutral drag effects on the LAGEOS and LARES satellites
- Solid and Ocean Tides on the LAGEOS and LARES satellites
- Precise Orbit Determination of the LAGEOS and LARES satellites
- Measurement of relativistic effects
- Conclusions and future work



The LARASE experiment and its goals

The LARASE goals:

- The **LAser RAnged Satellite Experiment (LARASE)** main goal is to provide accurate measurements for the gravitational interaction in the **weak-field** and **slow-motion** limit of **General Relativity** by means of a very precise laser tracking of geodetic satellites orbiting around the Earth (the two **LAGEOS** and **LARES**)
- Beside the quality of the tracking observations, guaranteed by the powerful **Satellite Laser Ranging (SLR)** technique of the **International Laser Ranging Service (ILRS)**, also the quality of the dynamical models implemented in the **Precise Orbit Determination (POD)** software plays a fundamental role in order to obtain precise and accurate measurements
- The models have to account for the perturbations due to both gravitational and non-gravitational forces in such a way to reduce as better as possible the difference between the *observed* range, from the tracking, and the *computed* one, from the models
- In particular, **LARASE** aims to improve the dynamical models of the current best laser-ranged satellites in order to perform a precise and accurate orbit determination, able to benefit also space geodesy and geophysics

The LARASE experiment and its goals

The LARASE activities:

1. Review of the literature, technical notes and all the documentation (**NASA, ALENIA, ASI**) related with the structure of the satellites and their physical characteristics
2. A reconstruction of the internal and external structure of the satellites with finite elements techniques
3. Review of the spin model of the two **LAGEOS** satellites and of their complex interaction with the Earth's magnetic field
4. Develop a spin model for **LARES**
5. Extension of the Yarkovsky–Schach thermal effect to the low spin-rate approximation
6. Impact of the neutral drag on the two **LAGEOS** satellites and on **LARES**
7. Solid and Ocean tides on the two **LAGEOS** satellites and on **LARES**
8. Precise Orbit Determination for the two **LAGEOS** satellites and for **LARES**

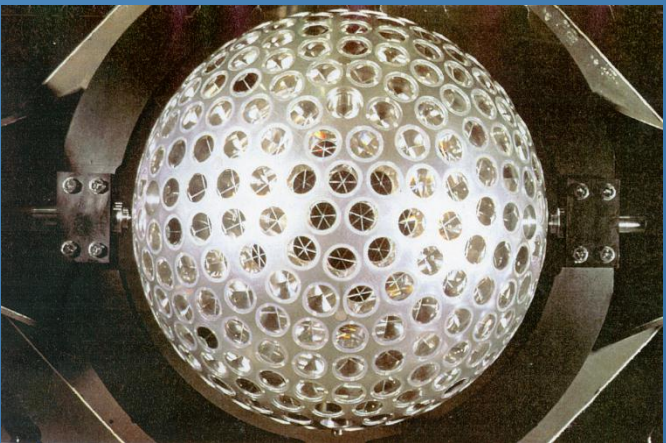


LAser **RE**lativity **S**atellite

The LARASE experiment and its goals

LAGEOS, LAGEOS II and LARES

orbit, size, mass and materials



LAser **GE**Odynamic **S**atellite
LAGEOS II

LAGEOS (NASA 1976)
LAGEOS II (NASA/ASI 1992)
LARES (ASI 2012)

Parameter		LARES	LAGEOS	LAGEOS II
a	[km]	7 828	12 270	12 163
e		0	0.004	0.014
I	[deg]	69.5	109.9	52.7
R	[cm]	18.2	30	30
M	[kg]	386.8	406.9	405.4
A/M	[m2/kg]	2.69·10 ⁻⁴	6.94·10 ⁻⁴	6.97·10 ⁻⁴

$$\left.\frac{A}{M}\right|_{Lares} \cong \frac{1}{2.6} \left.\frac{A}{M}\right|_{Lageos}$$

	LARES	LAGEOS
material	Tungsten	Al/Brass/Be/Cu
CCR (suprasil 311)	92	422 + 4
bin	30 s	120 s

The LARASE experiment and its goals

The two **LAGEOS** satellites and **LARES** are tracked with very high accuracy through the powerful **Satellite Laser Ranging (SLR)** technique

The **SLR** represents a very impressive and powerful technique to determine the round-trip time between Earth-bound laser Stations and orbiting passive (and not passive) Satellites

The time series of range measurements are then a record of the motions of both the end points: the Satellite and the Station (mm precision in the NP)

Thanks to the accurate modelling (of both gravitational and non-gravitational perturbations) of the orbit of these satellites — approaching 1 cm in range accuracy — we are able to determine their Keplerian elements with about the same accuracy

The precision of the measurement depends mainly on the laser pulse width, about $1 \cdot 10^{-10}$ s — $3 \cdot 10^{-11}$ s



The LARASE experiment and its goals

- Despite the smaller A/M ratio, the non-gravitational accelerations are not always smaller in magnitude for LARES with respect to LAGEOS II (or LAGEOS), due to the lower height (1450 vs. 5900 km) and the higher density of neutral atmosphere
- Being 50 times larger on LARES than on the two LAGEOS, the accurate modeling of neutral atmosphere drag needs special attention, because it might mask the presence of smaller and subtler effects

Effect	Estimate	LAGEOS II	LARES
Earth's monopole	$\frac{GM_{\oplus}}{r^2}$	2.69	6.51
Earth's oblateness	$3\frac{GM_{\oplus}}{r^2}\left(\frac{R_{\oplus}}{r}\right)^2\bar{C}_{2,0}$	-1.1×10^{-3}	-6.4×10^{-3}
Low-order geopotential harmonics	$3\frac{GM_{\oplus}}{r^2}\left(\frac{R_{\oplus}}{r}\right)^2\bar{C}_{2,2}$	5.4×10^{-6}	3.2×10^{-5}
High-order geopotential harmonics	$19\frac{GM_{\oplus}}{r^2}\left(\frac{R_{\oplus}}{r}\right)^{18}\bar{C}_{18,18}$	1.4×10^{-12}	4.6×10^{-9}
Moon perturbation	$2\frac{GM_{\oplus}}{r^3}r$	2.2×10^{-6}	1.4×10^{-6}
Sun perturbation	$2\frac{GM_{\odot}}{r_{\odot}^3}r$	9.6×10^{-7}	6.2×10^{-7}
General relativistic correction	$\frac{GM_{\oplus}}{r^2}\frac{GM_{\oplus}}{c^2}\frac{1}{r}$	9.8×10^{-10}	3.7×10^{-9}
Atmospheric drag	$\frac{1}{2}C_D\frac{A}{M}\rho V^2$	-2.6×10^{-13}	-1.3×10^{-11}
Solar radiation pressure	$C_R\frac{A}{M}\frac{\Phi_{\odot}}{c}$	3.2×10^{-9}	1.2×10^{-9}
Albedo radiation pressure	$C_R\frac{A}{M}\frac{\Phi_{\oplus}}{c}A_{\oplus}\left(\frac{R_{\oplus}}{r}\right)^2$	3.5×10^{-10}	2.4×10^{-10}
Thermal emission	$\frac{4}{9}\frac{A}{M}\frac{\Phi_{\oplus}}{c}\alpha\frac{\Delta T}{T_0}$	2.8×10^{-11}	not available
Dynamic solid tide	$3k_2\frac{GM_{\oplus}}{r}\left(\frac{R_{\oplus}}{r}\right)^2\frac{R_{\oplus}^3}{r^4}$	3.7×10^{-6}	2.2×10^{-5}
Dynamic ocean tide	~ 0.1 of the dynamic solid tide	3.7×10^{-7}	2.2×10^{-6}

Summary

- The LARASE experiment and its goals
- The internal structure of the LAGEOS and LARES satellites
- The rotational dynamics and the Spin Model for the LAGEOS and LARES satellites
- Neutral drag effects on the LAGEOS and LARES satellites
- Solid and Ocean Tides on the LAGEOS and LARES satellites
- Precise Orbit Determination of the LAGEOS and LARES satellites
- Measurement of relativistic effects
- Conclusions and future work



The internal structure of the LAGEOS and LARES satellites

Needed parameters:

Among the main parameters necessary to correctly model the dynamical behavior of an artificial satellite we have to consider:

- **its mass**
- **its center of mass position**
- **its moments of inertia**

If we look to the scientific literature and to the official documents (NASA, ASI, ALENIA) we can easily see a number of different values for these fundamental parameters, differences that we have mainly confined within the following categories:

1. **lack of complete measurements (hence of the flight model knowledge)**
2. **mistakes in information/popularization and its error propagation ...**
3. **material alloys and manufacturing tolerances**

The internal structure of the LAGEOS and LARES satellites

Needed parameters:

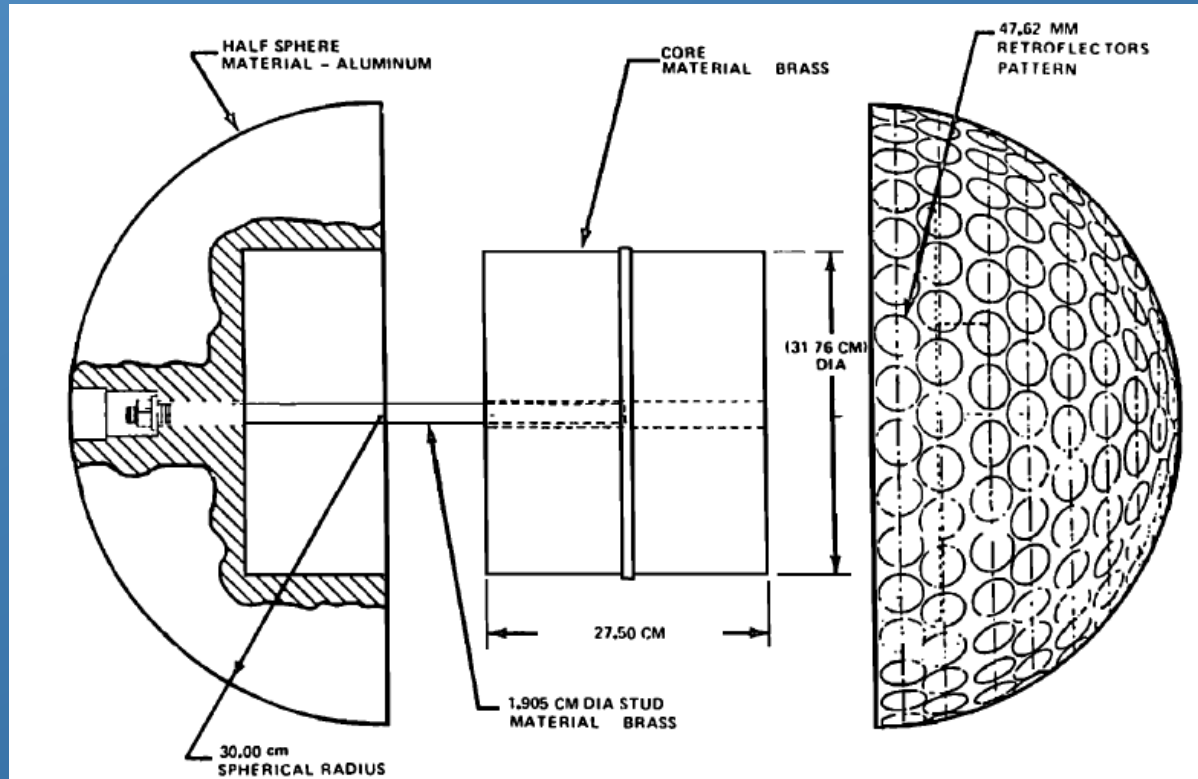
For instance, just to give an example, it is well known the controversy and the consequent very long debate about the material of the inner core of LAGEOS:

- **it is of BRASS (NASA-TN 1975; Cohen and Smith 1985) ?**
 - **it is of BERYLLIUM and COPPER (Johnson et al. 1976) ?**
- Still in Slabinski 1997 (more than 20 years after LAGEOS launch), it was reported Be-Cu for the core
- Only 10 years later Andrés concluded that the core was probably made of Brass as that of LAGEOS II, but probably with slightly different dimensions he has (wrongly) concluded

The internal structure of the LAGEOS and LARES satellites

Needed parameters:

A second and significant example are the correct dimensions for the stud and the core of LAGEOS: for instance, those reported in Cohen and Smith 1985 are wrong



The internal structure of the LAGEOS and LARES satellites

LARASE work: the satellites structure

From the analysis of all the documentation that we have been able to collect, we concluded that:

- the two LAGEOS have been built using almost identical working drawings
- and, if we exclude the different mounting of the Ge CCRs, the two satellites are almost identical (twins), being (slightly) different for manufacturing tolerances and material alloys

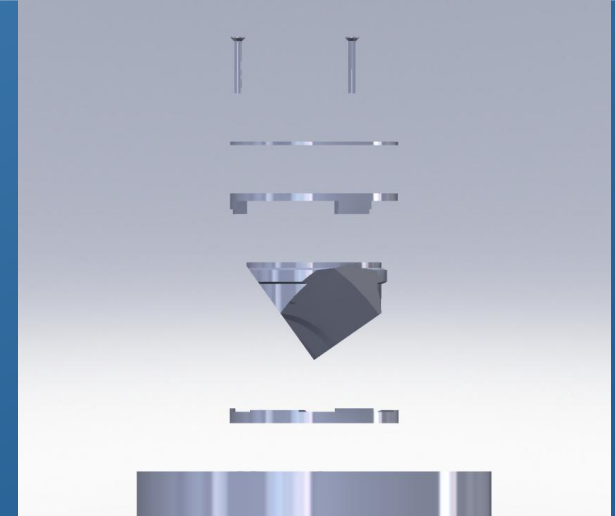
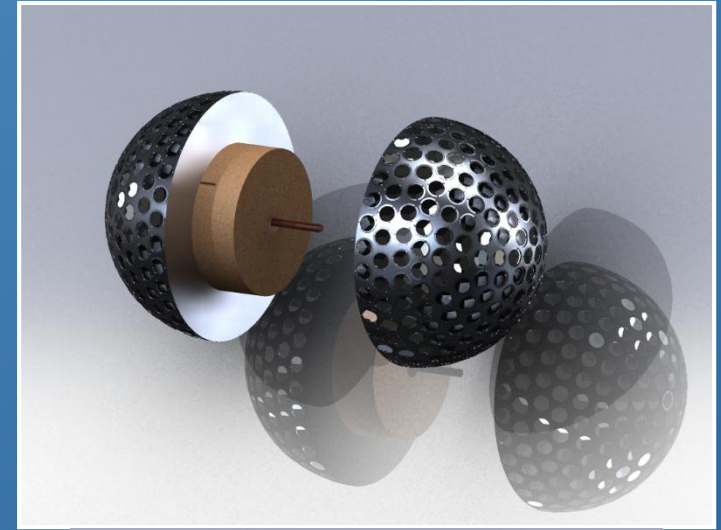
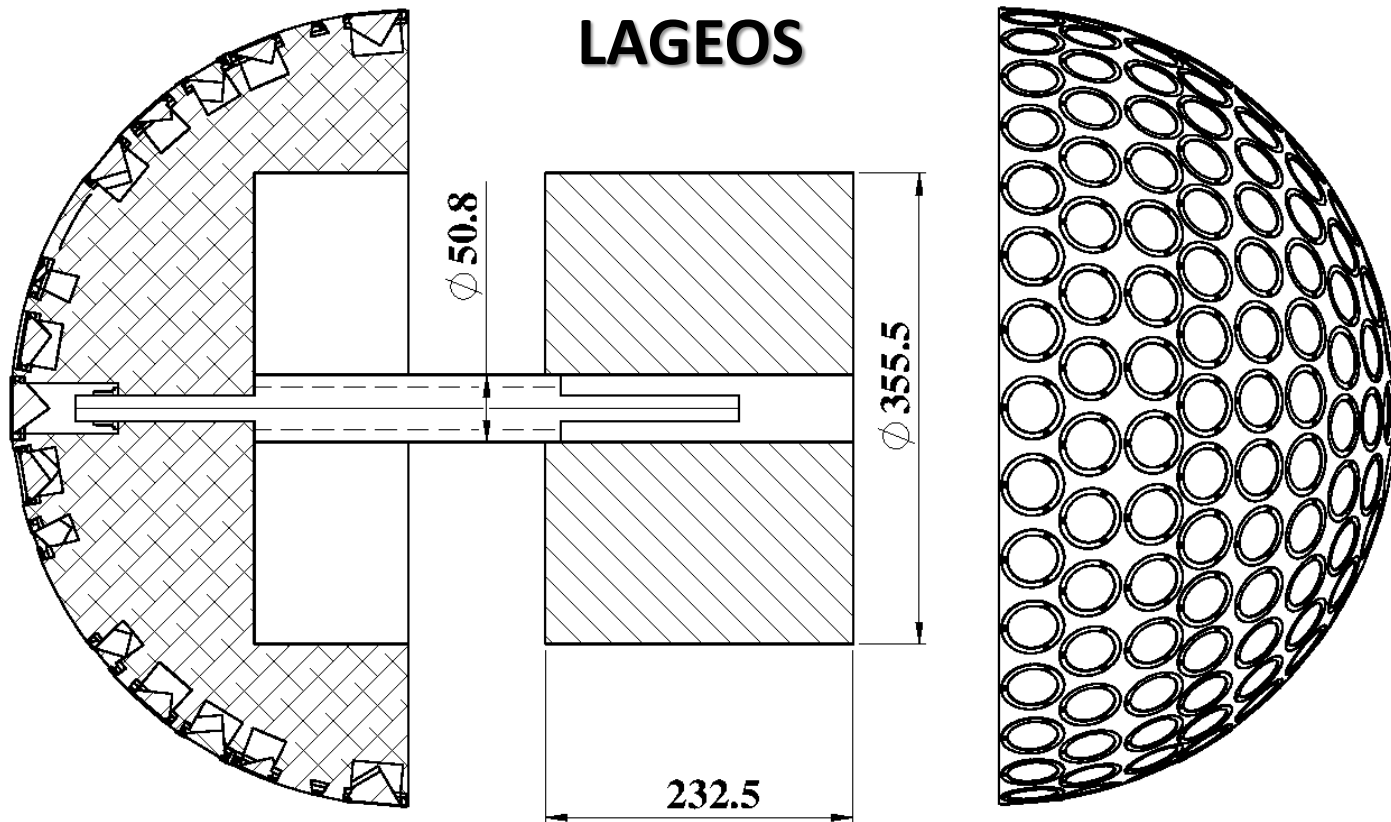
Therefore, we have been able to build a complete finite elements model of LAGEOS and LAGEOS II with SOLIDWORKS using:

- the working drawings of Minott et al. 1993
- the information about the involved materials as reported in Cogo 1988

The internal structure of the LAGEOS and LARES satellites

Restatement of the mass and moments of inertia of the two LAGEOS satellites

LARASE work: the satellites structure and dimensions



CCR

The internal structure of the LAGEOS and LARES satellites

LARASE work: the satellites structure and dimensions

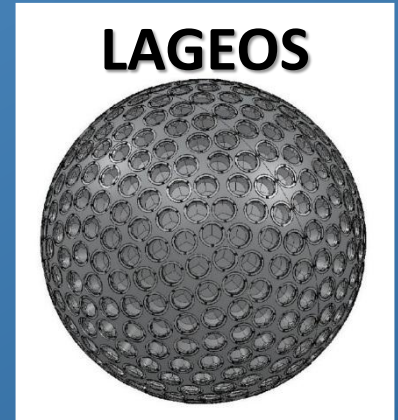


Table 1
Materials used for the construction of the two LAGEOS satellites (Cogo, 1988) and their nominal densities.

Satellite	Material density ρ_n (kg/m ³)		
	Hemispheres	Core	Stud
LAGEOS	AA6061 2700 ^a	QQ-B-626 COMP.11 8440 ^a	Cu-Be 8230 ^b
LAGEOS II	AlMgSiCu UNI 6170 2740 ^c	PCuZn39Pb2 UNI 5706 8280 ^c	Cu-Be QQ-C-172 8250 ^c

^a ASM International Handbook Committee (1990).

^b Bauccio (1993).

^c It is the value calculated in Cogo (1988) starting from the measured averaged composition.

The internal structure of the LAGEOS and LARES satellites

LARASE work: the satellites structure and dimensions

Table 2

Comparison of masses and moments of inertia for the two LAGEOS satellites. In the notation we follow [NASA \(1975\)](#). The x axis coincides (nominally) with the principal axis of inertia (the angle between the symmetry axis and the principal axis orientation was bound to be below 0.02 radians). Practically, this axis coincides with the initial rotation axis of the satellites.

Satellite origin of value	Mass (kg)	Moments of inertia (kg m ²)		
	M	I_{xx}	I_{yy}	I_{zz}
<i>LAGEOS flight arrangement</i>				
Computed value in NASA (1975)	409.8	11.516	11.084	11.084
Measured value in NASA (1975)	406.965	—	—	—
Values computed in the present work using nominal density of Table 1	405.93	11.40	10.93	10.93
<i>LAGEOS balance model</i>				
Computed value in NASA (1975)	440.3	13.14	12.71	12.71
Measured value in NASA (1975)	440.0	13.11	12.69	12.71
Value computed in the present work using nominal density of Table 1	437.68	13.09	12.62	12.62
Values computed in the present work using normalized density	440.00	13.16	12.68	12.68
<i>LAGEOS II flight arrangement</i>				
Computed values in Fontana (1990)	—	11.45	11.00	11.00
Measured value in Fontana (1990) , Fontana (1989) and Cogo (1988)	405.38	—	—	—
Values computed in the present work using nominal density of Table 1	404.97	11.44	10.99	10.99
<i>LAGEOS II without CCRs</i>				
Computed value in Fontana (1989)	386.59	10.39	9.95	9.95
Measured value in Fontana (1989)	387.20	9.67	9.37	9.15
Values computed in the present work using nominal density of Table 1	386.71	10.41	9.95	9.95
Values computed in the present work using normalized density	387.20	10.42	9.96	9.96

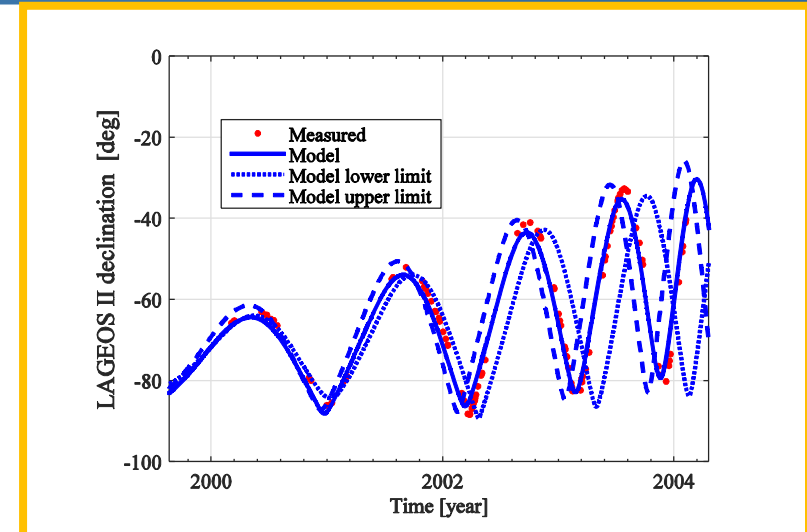
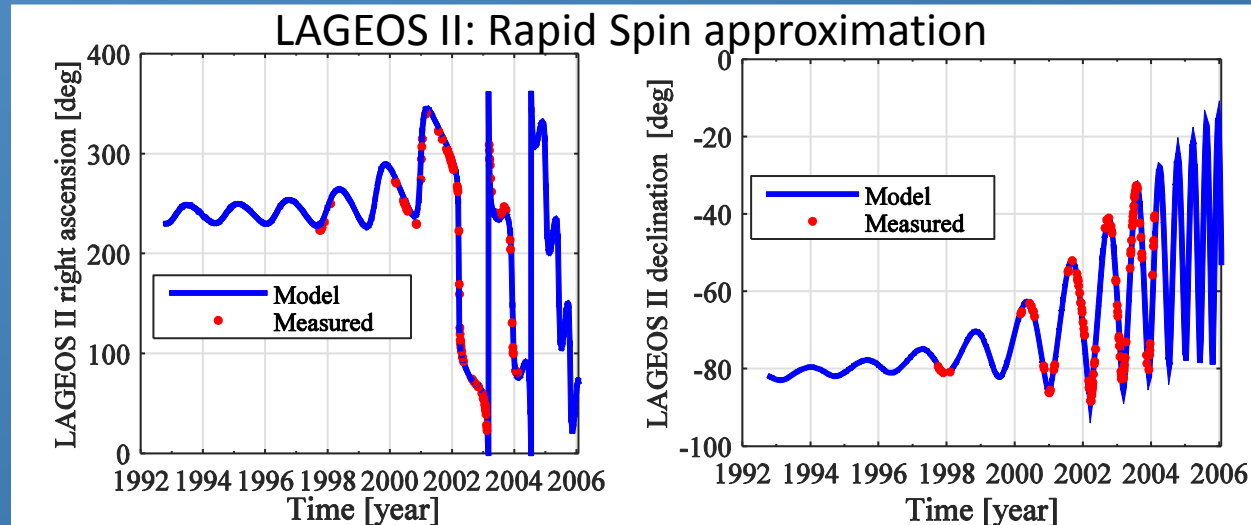
The internal structure of the LAGEOS and LARES satellites

LARASE work: the satellites structure and dimensions

Table 3


Mass and moments of inertia of LAGEOS and LAGEOS II to be used in the future. The masses are the one measured. The moments of inertia are those computed in the present work with normalized densities.


Satellite	Mass (kg) M	Moments of inertia (kg m^2)		
		I_{xx}	I_{yy}	I_{zz}
LAGEOS flight arrangement	406.97	11.42 ± 0.03	10.96 ± 0.03	10.96 ± 0.03
LAGEOS II flight arrangement	405.38	11.45 ± 0.03	11.00 ± 0.03	11.00 ± 0.03



The internal structure of the LAGEOS and LARES satellites

LARASE work: further details in the paper:


ELSEVIER


CrossMark

Available online at www.sciencedirect.com
ScienceDirect
Advances in Space Research 57 (2016) 1928–1938

**ADVANCES IN
SPACE
RESEARCH**
(a COSPAR publication)
www.elsevier.com/locate/asr

Review and critical analysis of mass and moments of inertia of the LAGEOS and LAGEOS II satellites for the LARASE program

Massimo Visco^{a,b}, David M. Lucchesi^{a,b,c,*}

^a *Istituto Nazionale di Astrofisica (INAF) – Istituto di Astrofisica e Planetologia Spaziali (IAPS), Via del Fosso del Cavaliere, 100, 00133 Roma, Italy*
^b *Istituto Nazionale di Fisica Nucleare (INFN), Sez. Tor Vergata, Via della Ricerca Scientifica 1, 00133 Roma, Italy*
^c *Istituto di Scienza e Tecnologia della Informazione (ISTI) – Consiglio Nazionale delle Ricerche (CNR), Via G. Moruzzi 1, 56124 Pisa, Italy*

Received 18 November 2015; received in revised form 8 February 2016; accepted 9 February 2016
Available online 15 February 2016

Abstract

The two LAGEOS satellites, currently the best tracked satellites by the stations of the International Laser Ranging Service (ILRS), play a significant role in the fields of space geodesy and geophysics as well as in very precise measurements and constraints in fundamental physics. Specifically, for the measurements of tiny relativistic effects it is mandatory to build accurate models for the dynamics of the satellites, in particular concerning their spin evolution and the determination of their temperature distribution and thermal behavior under different physical conditions. Consequently, an accurate knowledge of both the external and internal structure of the laser-ranged satellites, and of their main dynamic parameters to be used within the orbit models, is of crucial importance. In this work we reconstruct information about the structure, the materials used, and the moments of inertia of the two LAGEOS satellites. The moments of inertia of LAGEOS resulted to be $(11.42 \pm 0.03) \text{ kg m}^2$ for the cylindrical symmetry axis and $(10.96 \pm 0.03) \text{ kg m}^2$ for the other two main axes. The analogous quantities for LAGEOS II are $(11.45 \pm 0.03) \text{ kg m}^2$ and $(11.00 \pm 0.03) \text{ kg m}^2$. We also built a 3D-CAD model of the satellites structure which is useful for finite element-based analysis. We tried to solve contradictions and overcome several misunderstanding present in the historical literature of the older LAGEOS, carefully reanalyzing the earlier technical papers. To test the results we obtained, we used our moments of inertia to compute the spin evolution of the two satellites obtaining a good agreement between measured and estimated values for the spin direction and the rotational period. We believe we now have accurate knowledge of the mass, moments of inertia, and composition of both LAGEOS satellites.

© 2016 COSPAR. Published by Elsevier Ltd. All rights reserved.

Summary

- The LARASE experiment and its goals
- The internal structure of the two LAGEOS satellites
- The rotational dynamics and the Spin Model for the LAGEOS and LARES satellites
- Neutral drag effects on the LAGEOS and LARES satellites
- Solid and Ocean Tides on the LAGEOS and LARES satellites
- Precise Orbit Determination of the LAGEOS and LARES satellites
- Measurement of relativistic effects
- Conclusions and future work



The rotational dynamics and the Spin Model for a satellite

Spin Models

The rotational dynamics of a satellite represents a very important issue that deeply impacts the goodness of the orbit modelling

Indeed, the modelling of several disturbing effects (like the thermal thrust ones) depends on the knowledge of the spin period and orientation in the inertial space:

1. Yarkovsky–Schach effect
2. Earth–Yarkovsky (Rubincam) effect
3. Asymmetric reflectivity from the satellite surface

Their modelling will greatly improve the POD of the two LAGEOS satellites avoiding the current (and significant) use of empirical accelerations during the data reduction

The rotational dynamics and the Spin Model for a satellite

Past Spin Models

The best spin models developed in the past are:

1. Bertotti and Iess (JGR 96 B2, 1991)
 2. Habib et al. (PRD 50, 1994)
 3. Farinella, Vokrouhlicky and Barlier (JGR 101, 1996); Vokrouhlicky (GRL 23, 1996)
 4. Andrés, 1997 (PhD Thesis) and LOSSAM
- All of these studies, with the exception of Habib et al., attack and solve the problem of the evolution of the rotation of a satellite in a terrestrial inertial reference system, in the so-called rapid spin approximation and they introduce equations for the external torques that are averaged over time;
 - Their fit to the spin observations was good, especially in the case of the LOSSAM model for the LAGEOS II satellite;
 - Habib et al. use a body-fixed reference system and non-averaged torques; their model does not fit so well the observations.

The rotational dynamics and the Spin Model for a satellite

LARASE Spin Model

We have deeply reviewed previous spin models, in particular we:

- first built our own spin model in the rapid spin approximation
- adopted non-averaged torques in the equations to describe the slow spin approximation: we solved the problem of a metallic sphere rotating in an alternate magnetic field
- introduced in the equations all known possible torques (like in LOSSAM model)
- solved the equations in a body-fixed reference system in order to better describe the misalignment between the symmetry axis and the spin
- included in the equations the terms due to the transversal asymmetry
- carefully studied the satellites moments of inertia

The LARASE models, ‘rapid-spin’ model and ‘general model’, are well consolidated

The rotational dynamics and the Spin Model for a satellite

LARASE Spin Model: the involved torques

We consider in the case of the two LAGEOS satellites four torques:

1. The magnetic torque (eddy currents)

$$\begin{aligned} M_{mag}^E = & V \sum_{i=1}^9 \frac{|B_i|^2}{2|\omega_s|} \{ A_i'' [1 + \cos(2\omega_i t + 2\varphi_i)] - D_i' \sin(2\omega_i t + 2\varphi_i) \} \omega_s + \\ & V \sum_{i=1}^9 \frac{B_i \cdot \omega_s}{2|\omega_s|^2} \{ [\alpha'(\omega_i) - A_i'] [1 + \cos(2\omega_i t + 2\varphi_i)] - [D_i'' + \alpha''(\omega_i)] \sin(2\omega_i t + 2\varphi_i) \} (\omega_s \times B_i) + \\ & V \sum_{i=1}^9 \frac{B_i \cdot \omega_s}{2|\omega_s|} \{ -A_i'' [1 + \cos(2\omega_i t + 2\varphi_i)] + D_i' \sin(2\omega_i t + 2\varphi_i) \} B_i \end{aligned}$$

2. The gravitational torque

$$M_{grav}^b = 3\omega_{\oplus}^2 \{ \hat{s}^b \times [I_x(\hat{s}^b \cdot \hat{x}^b) \hat{x}^b + I_y(\hat{s}^b \cdot \hat{y}^b) \hat{y}^b + I_z(\hat{s}^b \cdot \hat{z}^b) \hat{z}^b] \}$$

3. The asymmetric reflectivity torque (C_R differences)

$$M_{ar}^b = \nu \frac{2}{3} \rho^3 \frac{\Phi}{c} \Delta\rho C_R (\hat{z}^b \times \hat{s}_{\odot}^b) |\hat{z}^b \times \hat{s}_{\odot}^b|$$

4. The CoM offset torque (with respect to the center of geometry)

$$M_{off}^b = \nu \pi \rho^2 \frac{\Phi}{c} C_R (h^b \times \hat{s}_{\odot}^b)$$

$$\frac{d\vec{L}}{dt} = \underbrace{M_{mag} + M_{grav}} + M_{ar} + M_{offset}$$

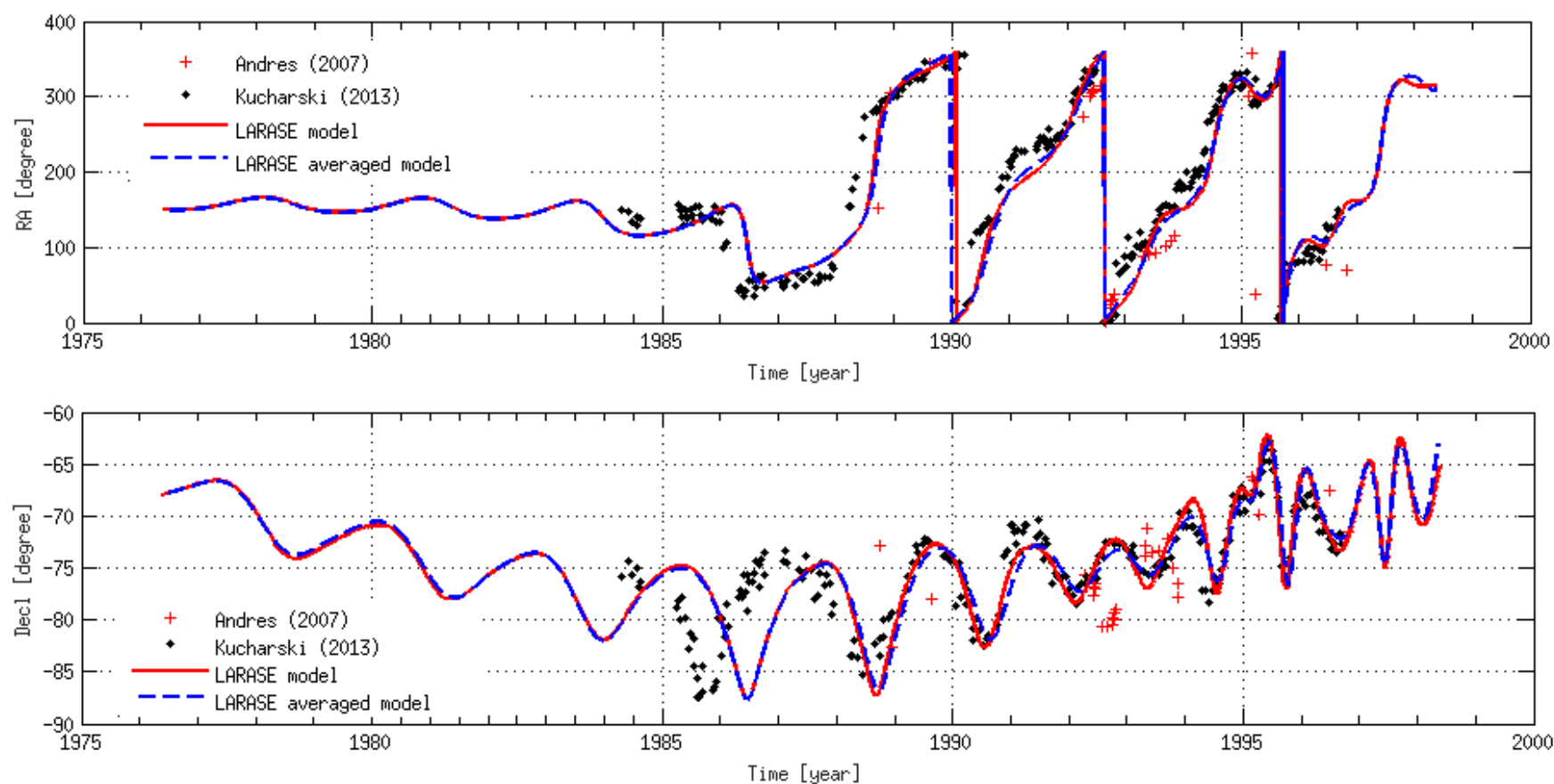
Angular momentum evolution

These two are the most important to consider

The rotational dynamics and the Spin Model for a satellite

LARASE Spin Model: preliminary results for LAGEOS

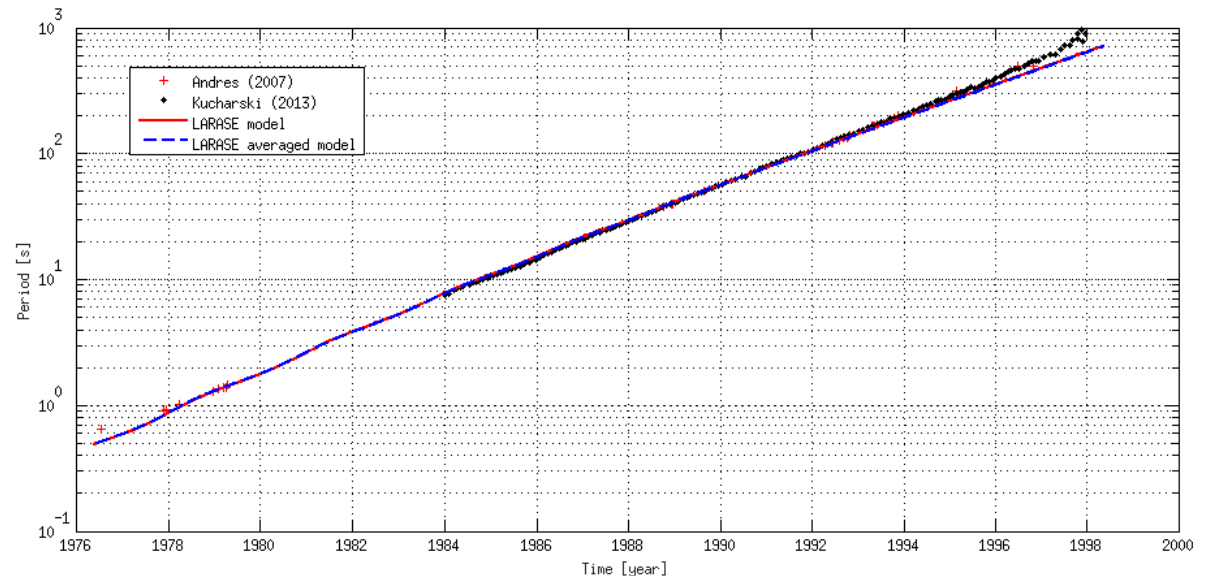
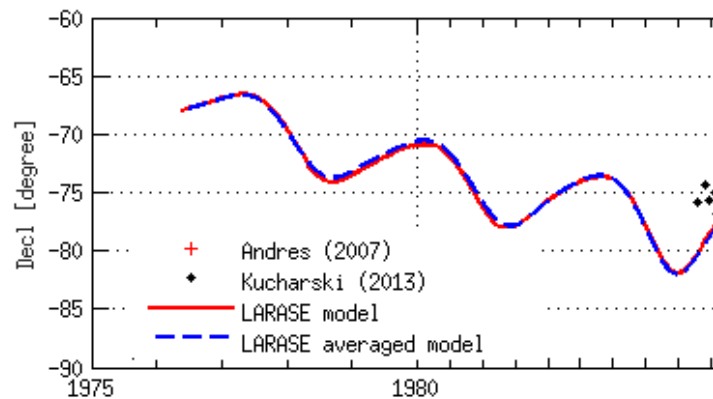
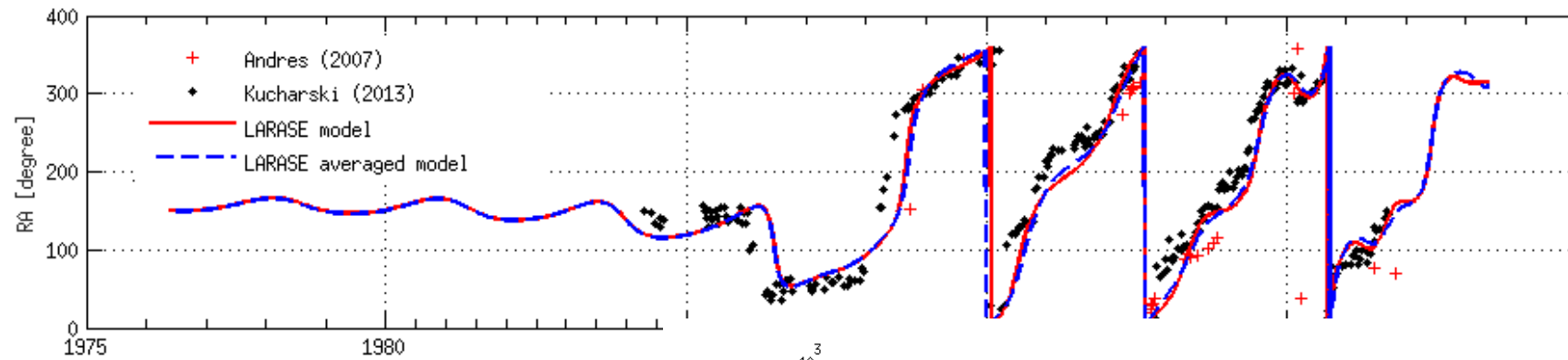
Blue = LARASE model for the rapid-spin
Orange = LARASE general model



The rotational dynamics and the Spin Model for a satellite

LARASE Spin Model: preliminary results for LAGEOS

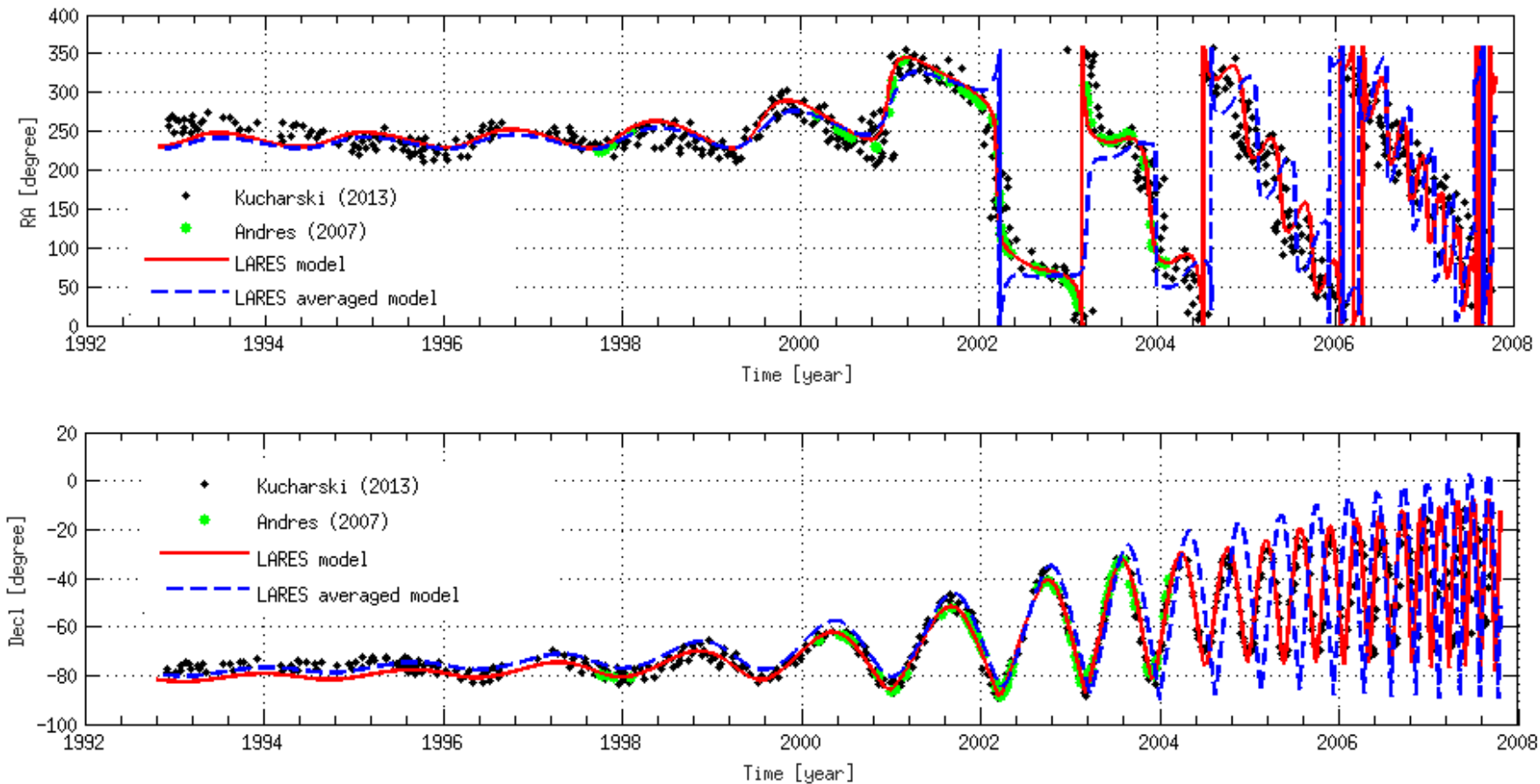
Blue = LARASE model for the rapid-spin
Orange = LARASE general model



The rotational dynamics and the Spin Model for a satellite

LARASE Spin Model: preliminary results for LAGEOS II

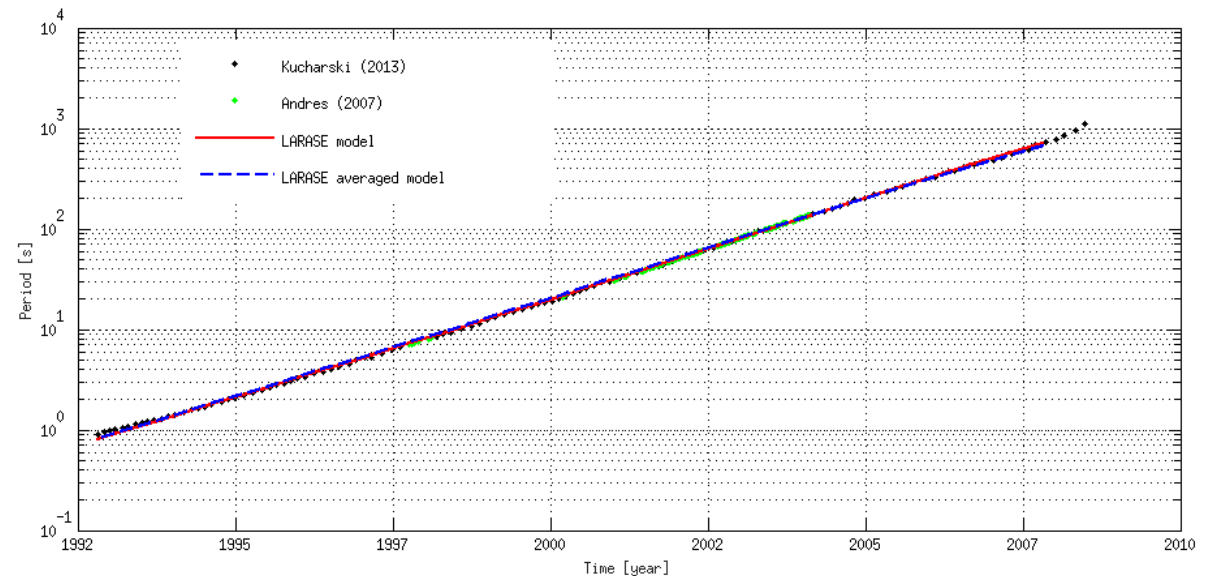
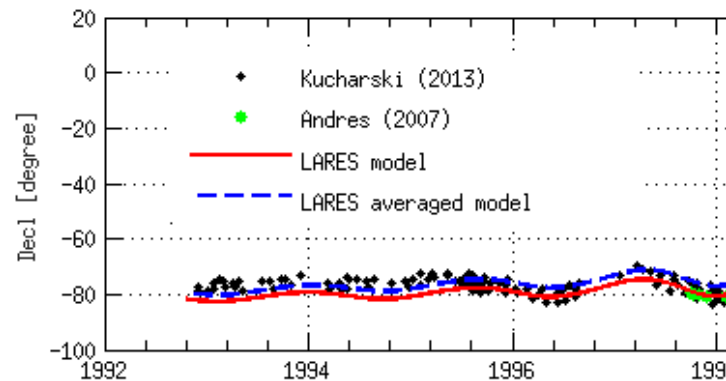
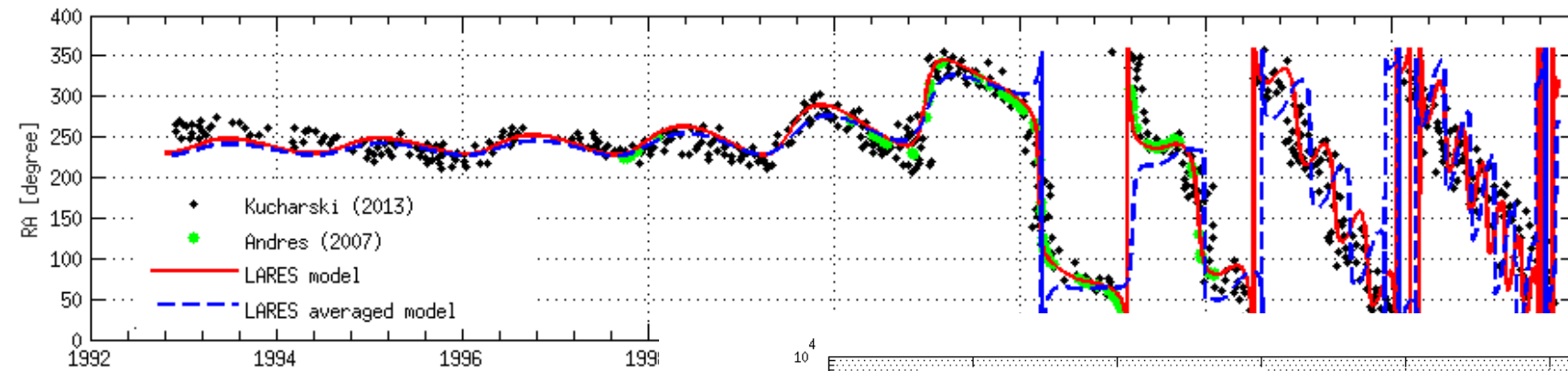
Blue = LARASE model for the rapid-spin
Orange = LARASE general model



The rotational dynamics and the Spin Model for a satellite

LARASE Spin Model: preliminary results for LAGEOS II

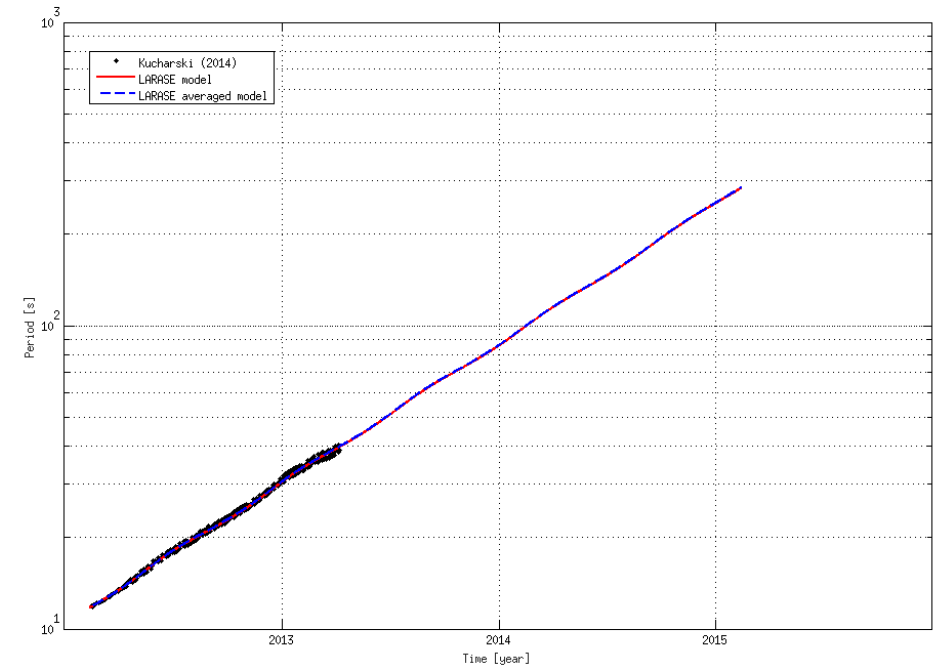
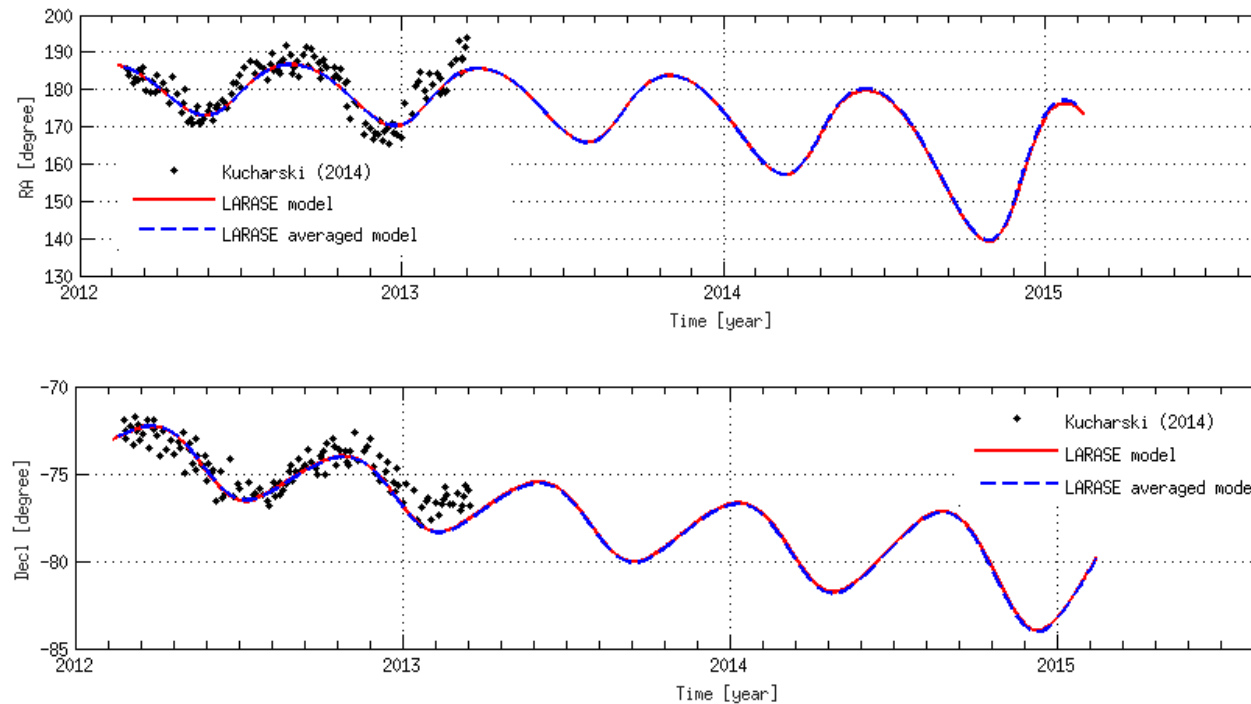
Blue = LARASE model for the rapid-spin
Orange = LARASE general model



The rotational dynamics and the Spin Model for a satellite

LARASE Spin Model: preliminary results for LARES

Blue = LARASE model for the rapid-spin
Orange = LARASE general model



- The spin evolution is almost due to the magnetic torque
- The gravitational torque is almost null, we fit the data with an oblateness of about:

$$\frac{C - A}{C} < 10^{-4}$$

Kucharski et al., IEEE Geos. Rem. Sens. Lett. 11, 2014

$$T \cong P_{\text{orb}} \cong 115 \text{ min. after } \cong 5.9 \text{ years}$$

$$T(\text{s}) \cong 11.8 \cdot e^{D/341} \quad D [\text{days}]$$

Summary

- The LARASE experiment and its goals
- The internal structure of the two LAGEOS satellites
- The rotational dynamics and the Spin Model for the LAGEOS and LARES satellites
- Neutral drag effects on the LAGEOS and LARES satellites
- Solid and Ocean Tides on the LAGEOS and LARES satellites
- Precise Orbit Determination of the LAGEOS and LARES satellites
- Measurement of relativistic effects
- Conclusions and future work



Neutral drag effects on the LAGEOS and LARES satellites

Why study and modelling the Drag?

LAGEOS and LAGEOS II

In the case of the two **LAGEOS** satellites, the RMS of the range residuals is at the cm level; this means that once modelled and removed the perturbations due to the thermal effects, in particular that from the **Yarkovsky–Schach** effect, we are able (in principle) to extract, from the residuals of the satellites, a direct information of the impact of the drag on the orbit and, consequently, of the characteristics of the atmosphere at the altitude (~5900 km) and inclination (~110°/ ~53°) of the satellites

Indeed, from the expression of the along-track displacement we obtain:

$$\Delta s \cong \frac{3}{2} a \Delta t^2 \quad \begin{matrix} \Delta s \cong 1cm \\ \Delta t \cong 14days \end{matrix} \longrightarrow a \cong 5 \cdot 10^{-15} m/s^2$$

Which is about 1/100 of the order-of-magnitude of the along-track acceleration as produced from a simplified model of the neutral drag perturbation

Neutral drag effects on the LAGEOS and LARES satellites

Why study and modelling the Drag?

LAGEOS and LAGEOS II

Such a result, if reached, will be very important because it represents the first step to study and separate the effects of the two typologies of drag provoked from the interaction of the satellite surface with its environment, i.e.:

1. drag from neutral particles: collisions
 2. drag from charged particles: Coulomb interaction + collisions
- In the case of **LARES**, the impact of the drag on the orbit is larger because of the much lower height of the satellite with respect to that of the two **LAGEOS's** (1450 km vs 5900 km)
 - the impact is in part mitigated by the lower area/mass ratio of the satellite

Neutral drag effects on the LAGEOS and LARES satellites

LARASE activities

We took advantage of the use of the software **SATRAP** (**SAT**ellite **Re**-entry **A**nalysis **P**rogram), that is able to load several different models for the Earth's atmosphere together with the geomagnetic and solar activities indices while using the following dynamical models for the orbit propagation:

1. Earth's geopotential
2. Luni-solar perturbations
3. Solar radiation pressure and eclipses
4. Neutral drag

Neutral drag effects on the LAGEOS and LARES satellites

LARASE activities

Density models implemented in **SATRAP**:

1. Vandenberg AFB reference atmosphere 1971 (**VRA-71**): < 86 km
2. United States Standard Atmosphere 1976 (**USSA-76**): 86 km – 1000 km
3. Thermospheric total Density 1988 (**TD-88**): 150 km – 750 km
4. Jacchia-Roberts 1971 (**JR-71**): 125 km – 2500 km
5. Mass Spectrometer and Incoherent Scatter 1986 (**MSIS-86**): 85 km – 3000 km
6. Mass Spectrometer and Incoherent Scatter Radar Extended 1990 (**MSISE-90**): 0 km – 3000 km
7. Naval Research Laboratory MSISE 2000 (**NRLMSISE-00**): 0 km – 3000 km
8. Empirical Russian model **GOST-2004**: 0 km – 1500 km
9. Jacchia-Bowman 2006 (**JB2006**): 120 km – 4000 km
10. Jacchia-Bowman 2008 (**JB2008**): 120 km – 4000 km

Neutral drag effects on the LAGEOS and LARES satellites

LARASE activities

In particular, the following activities have been started concerning the impact of the neutral drag perturbations on the satellites orbit:

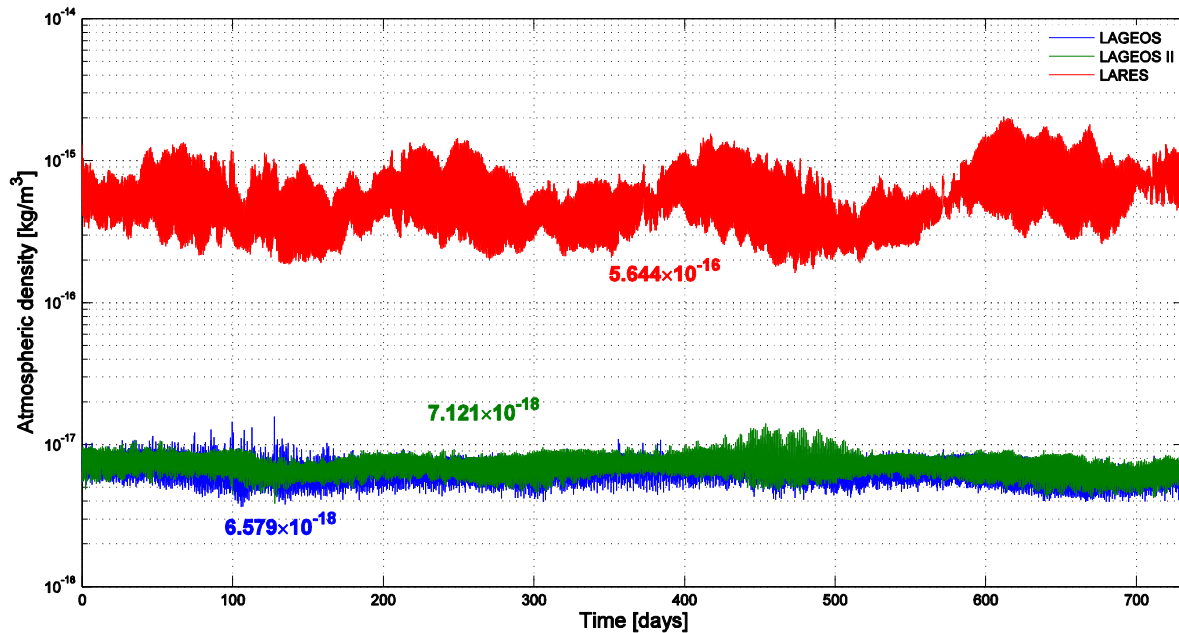
1. comparison of the different models at the satellites altitude
2. estimate of the perturbing accelerations in the MOD and RTW reference systems
3. estimate of the disturbing effects on the orbital elements of the satellites
4. estimate of the satellites physical C_D (role of Ajisai as a calibrator in the case of LARES)

We jointly use **SATRAP** with **GEODYN** in order to exploit as better as possible their characteristics:

1. for instance, the perturbing accelerations in the RTW reference systems may be used as empirical accelerations in **GEODYN** during a data reduction

Neutral drag effects on the LAGEOS and LARES satellites

LARASE activities: Atmospheric density comparison at the altitudes of the satellites and the average transversal accelerations



	LAGEOS	LAGEOS 2	LARES
$T \text{ [m/s}^2\text{]}$	-3.111×10^{-13}	-2.613×10^{-13}	-1.219×10^{-11}
$\sigma \text{ [m/s}^2\text{]}$	0.665×10^{-13} [21%]	0.5195×10^{-13} [20%]	0.1295×10^{-11} [11%]

$$T_{Lares} \approx 40 \cdot T_{Lageos}$$
$$T_{Lares} \approx 47 \cdot T_{Lageos2}$$

despite $\left. \frac{A}{M} \right|_{Lares} \cong \frac{1}{2.6} \left. \frac{A}{M} \right|_{Lageos}$

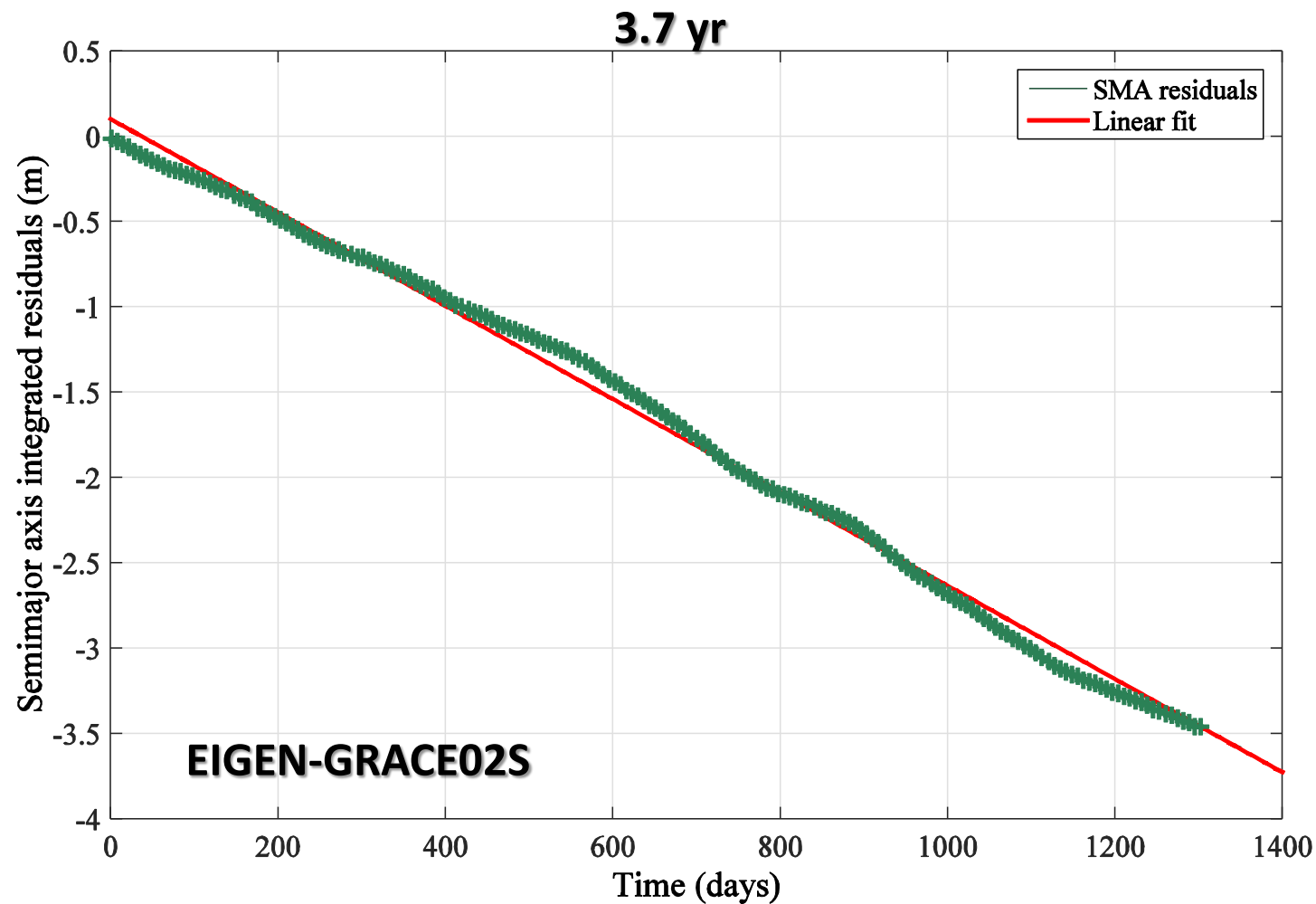
Neutral drag effects on the LAGEOS and LARES satellites

On the observed orbital decay of LARES semi-major axis (SMA)

- From a **POD** of **LARES** over a time span of about **3.7 years**, we have been able to measure a mean orbital decay in the residuals of its semi-major axis of about **−1 m per year**, i.e. −2.74 mm per day
- This **POD** has been obtained analyzing the **LARES** normal points with the **GEODYN II** (NASA/GSFC) software and the **EIGEN-GRACE02S** model for the Earth's gravitational field
- Neither the neutral and charged atmosphere drag, nor the thermal effects, have been included in the dynamical models
- The corresponding unmodeled mean transversal acceleration of about $-1.444 \times 10^{-11} \text{ m/s}^2$ then includes all the effects of the perturbations not taken into account in the **POD** and eventually giving a secular and/or long-period contribution to the transversal acceleration component
- The first line of attack was therefore the accurate modeling of neutral atmosphere drag, in order to evaluate how much of the unaccounted for acceleration can be explained by current thermospheric density models

Neutral drag effects on the LAGEOS and LARES satellites

On the observed orbital decay of LARES semi-major axis (SMA)



Decay of **LARES** semi-major axis residuals (green) as obtained by **GEODYN II** over a time span of about **3.7 yr** and its best fit with a straight line (red).

The observed decay of LARES semi-major axis residuals is **0.9988 m/yr** (i.e., about 2.7 mm/day!).

$$\langle T \rangle \cong -1.444 \times 10^{-11} \frac{m}{s^2}$$

Neutral drag effects on the LAGEOS and LARES satellites

Detailed drag modelling

- A modified version of the **SATRAP** tool, developed at ISTI/CNR, was used to compute the neutral drag acceleration acting on **LARES**, as a function of time, taking into account the real evolution of solar and geomagnetic activities and the observed secular semi-major axis decay
- The following thermospheric density models were used within SATRAP to compute the components of the neutral drag acceleration in the reference system R (Radial), T (Transverse) and W (Out-of-Plane): **JR-71, MSIS-86, MSISE-90, NRLMSISE-00 and GOST-2004**
- The analysis covered the first **3.7** years of **LARES** in orbit and **the drag coefficient C_D was adjusted, for each atmospheric density model, in order to reproduce the average decay of the semi-major axis by -0.9988 m/year**, obtained through the analysis of the residuals of the GEODYN II precise orbit determination

Neutral drag effects on the LAGEOS and LARES satellites

Summary of the results for LARES

- For each thermospheric density model used in the analysis, the following mean adjusted drag coefficients were obtained, in order to reproduce the observed semi-major axis decay of LARES over the first 3.7 years of flight:
 - JR-71 $\rightarrow \langle C_D \rangle = 3.95$
 - MSIS-86 $\rightarrow \langle C_D \rangle = 3.71$
 - MSISE-90 $\rightarrow \langle C_D \rangle = 3.73$
 - NRLMSISE-00 $\rightarrow \langle C_D \rangle = 3.78$
 - GOST-2004 $\rightarrow \langle C_D \rangle = 4.21$
- The average drag coefficient among the 5 models was **3.88**, with a maximum discrepancy of 8.6%, but MSIS-86, MSISE-90 and NRLMSISE-00 have a common heritage and are very similar
- Taking the average between JR-71, NRLMSISE-00 and GOST-2004, the mean drag coefficient resulted to be **3.98**, with a maximum discrepancy of 5.8%
- The differences are well below the intrinsic uncertainties of the models, around 15% (or more)

Neutral drag effects on the LAGEOS and LARES satellites

- The results outlined strongly support the conclusion that most of the observed secular semi-major axis decay of LARES is due to neutral atmosphere drag
- This conclusion is fully consistent with the predictions, uncertainties and range of applicability of some of the best thermospheric density models available and used by the orbital dynamics community
- It is further strengthened by the totally independent results obtained with AJISAI, a spherical satellite orbiting at a similar altitude, but with quite different construction and surface properties, leading to a different response to non-gravitational perturbations
- Contrary to what is happening in the case of LAGEOS and LAGEOS II, where neutral atmosphere drag accounts for less than 10% of the observed semi-major axis decay (≈ -0.2 m/year), for LARES it is a major player among non-gravitational perturbations and its secular, long-term and short-term signatures must be investigated and modeled in detail, in order to reliably detect and characterize other comparable, or smaller (depending on the RTW component), perturbing accelerations
- The work carried out on neutral atmosphere drag was just one of several aspects addressed in the framework of LARASE to deeply understand and evaluate all error sources affecting the primary and secondary goals of the experiment
- It made possible to check and validate independently the conditions of applicability of the atmospheric density models implemented in GEODYN II
- A detailed signature analysis is ongoing to characterize the various models, for instance the Russian GOST-2004 vs. the American JR-71 and NRLMSISE-00
- Due to the absolute prevalence of neutral drag on LARES, this work is very important for the reliable identification and characterization of smaller non-gravitational perturbations, easily masked by the large thermospheric drag signal
- All taken into account, an along-track unmodeled acceleration with a mean value of $\underline{-2.1 \times 10^{-13} \text{ m/s}^2}$ (i.e. less than 1.5% of neutral atmosphere drag) was identified in the POD residuals of GEODYN II, probably attributable to thermal drag
- Ciufolini et al. (2015) have found a residual along-track acceleration of about $\underline{-4 \times 10^{-13} \text{ m/s}^2}$ (Eur. Phys. J. Plus 130, 133)

Summary

- The LARASE experiment and its goals
- The internal structure of the two LAGEOS satellites
- The rotational dynamics and the Spin Model for the LAGEOS and LARES satellites
- Neutral drag effects on the LAGEOS and LARES satellites
- Solid and Ocean Tides on the LAGEOS and LARES satellites
- Precise Orbit Determination of the LAGEOS and LARES satellites
- Measurement of relativistic effects
- Conclusions and future work



Tides on the LAGEOS satellites and on LARES

Tides are important to be modelled because they perturb the orbit of a satellite under three main effects:

1. Kinematic: because they produce a periodic pulsation of the Earth and of the on-ground stations
 2. Dynamic: because they cause a time variation of the geopotential that affects the orbit
 3. Reference System: because they perturb the Earth rotation thus affecting the reference systems used in the orbit computation
- Solid tides account for about 90% of the Moon and Sun tidal disturbing potential, and are responsible for the larger tidal effects on the orbit of a satellite.
 - Ocean tides are difficult to be modelled because of the greater complexity of the phenomena involved and their uncertainties are a factor of 10 larger than those of solid tides

Tides on the LAGEOS satellites and on LARES

Impact of Earth's Solid zonal and tesseral tides on the node of the two LAGEOS and LARES

$$\Delta\Omega_f = \frac{g_{\oplus}}{na^2\sqrt{1-e^2}\sin i} \sum_{m=0}^{\ell} \left(\frac{R_{\oplus}}{a}\right)^{\ell+1} A_{\ell m} \sum_{p=0}^{+\infty} \sum_{q=-\infty}^{+\infty} \frac{dF_{\ell mp}}{di} G_{\ell pq} \frac{k_{\ell m}^f H_{\ell}^m}{f_I}$$

Zonal tides: $\ell = 2, m=0$

Tide	Period	LAGEOS	LAGEOS II	LARES
055.565	6798.38	-1080.22	1976.46	5332.68
055.575	3399.19	-5.23	9.57	25.81
056.554 S_a	365.25	9.97	-18.24	-49.20
057.555 S_{sa}	182.625	31.15	-56.99	-153.75

The tidal amplitudes are in mas

(+) refers to westward tidal waves

(-) refers to eastward tidal waves

Tesseral tides: $\ell = 2, m=1$

Tide	Period	LAGEOS	Period	LAGEOS II	Period	LARES
165.545	1232.95	-40.95	-525.23	7.33	-225.77	35.74
165.555 K_1	1043.67	1738.57	-569.21	-398.25	-223.53	-1853.77
165.565	904.77	202.12	-621.22	-58.29	-241.84	-257.44
163.555 P_1	-221.36	135.76	-138.26	35.62	-102.48	299.51

In the case of the LARES satellite the amplitudes are much larger than those of the two LAGEOS satellites

Tides on the LAGEOS satellites and on LARES

Impact of Earth's Ocean tides on the node of the two LAGEOS and LARES

$$\Delta\Omega_f = \frac{1}{na^2\sqrt{1-e^2}\sin i} \sum_{m=0}^{\ell} \sum_{+}^{-} \left(\frac{R_{\oplus}}{a}\right)^{\ell+1} A_{\ell mf}^{\pm} \sum_{p=0}^{\ell} \sum_{q=-\infty}^{+\infty} \frac{dF_{\ell mp}}{di} G_{\ell pq} \frac{1}{f_p}$$

$$\ell = 2, p = 1, q = 0$$

The tidal amplitudes are in mas

(+) refers to westward tidal waves

(-) refers to eastward tidal waves

Tide	LAGEOS		LAGEOSII		LARES	
Doodson number	Period [days]	Amplitude [mas]	Period [days]	Amplitude [mas]	Period [days]	Amplitude [mas]
065.455 (M_m)	27.55	-0.53	27.55	0.97	27.55	2.62
056.554 (S_a)	365.25	-21.47	365.25	39.30	365.25	106.40
075.555 (M_f)	13.66	-0.62	13.66	1.14	13.66	3.08
057.555 (S_{sa})	182.62	-6.52	182.62	11.94	182.62	32.32
165.555 (K_1)	1043.67	162.30	-569.21	-37.23	-233.53	-173.64
163.555 (P_1)	-221.36	-11.59	-138.26	-3.05	-102.48	-25.66
145.555 (O_1)	-13.84	-1.90	-13.34	-0.77	-12.91	-8.45
135.655 (Q_1)	-9.21	-0.29	-8.99	-0.12	-8.79	-1.31
275.555 (K_2)	521.835	-7.18	-284.61	-7.17	-116.77	-7.96
273.555 (S_2)	-280.95	14.84	-111.24	-10.75	-71.23	-18.63

In the case of the LARES satellite the amplitudes are much larger than those of the two LAGEOS satellites

Summary

- The LARASE experiment and its goals
- The internal structure of the two LAGEOS satellites
- The rotational dynamics and the Spin Model for the LAGEOS and LARES satellites
- Neutral drag effects on the LAGEOS and LARES satellites
- Solid and Ocean Tides on the LAGEOS and LARES satellites
- Precise Orbit Determination of the LAGEOS and LARES satellites
- Measurement of relativistic effects
- Conclusions and future work



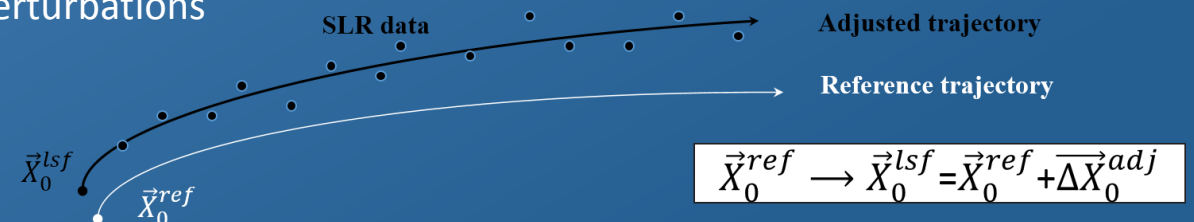
Precise Orbit Determination

For a precise orbit determination (POD) three main ingredients are needed:

1. **very good observations** [SLR data provided by International Laser Ranging Service (ILRS)]
2. **very good models: dynamical models, reference frames** (we follow the IERS Conventions)
3. **and a dedicated software for the data reduction** [GEODYN II (NASA/GSFC)]

The way in which **GEODYN II** works is composed (substantially) of two parts:

1. **the orbit prediction problem**
 2. **and the parameter estimation problem**
- It is well known from space geodesy techniques that it is not possible to solve for a pure deterministic orbit of a spacecraft when long-arc analyses are performed
 - It is necessary to decompose the long-arc in a number of shorter arcs, not causally connected, and solve (by means of a least-squares-fit) for the initial conditions of the satellite state-vector (position and velocity) for each arc, together with a set of parameters in order to absorb unmodelled or poorly modelled perturbations



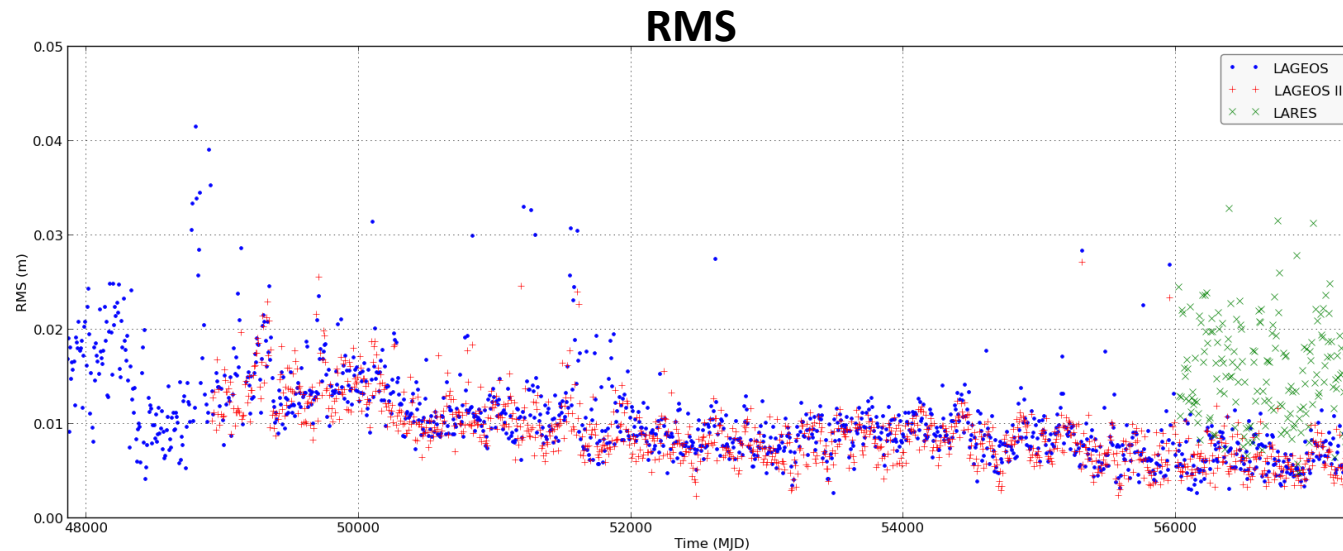
Precise Orbit Determination

Models implemented in the orbital analysis of LAGEOS's satellites

Geopotential (static part)	JGM-3; EGM96; EIGEN2S; EG02S;CHAMP; GRACE
Geopotential (tides)	Ray GOT99.2
Lunisolar + Planetary Perturbations	JPL ephemerides DE-403
General relativistic corrections	PPN
Direct solar radiation pressure	Cannonball model
Albedo radiation pressure	Knocke-Rubincam model
Yarkovsk –Schach effect	Afonso et al., 1980, Farinella –Vokrouhlicky 1996
Earth–Yarkovsky effect	Rubincam 1987 – 1990 model
Spin–axis evolution	Farinella et al., 1996 model, LARASE (2014) model
Stations position	ITRF2000; ITRF 2008
Ocean loading	Scherneck model (with GOT99.2 tides)
Polar motion	IERS (estimated)
Earth rotation	VLBI + GPS

Precise Orbit Determination

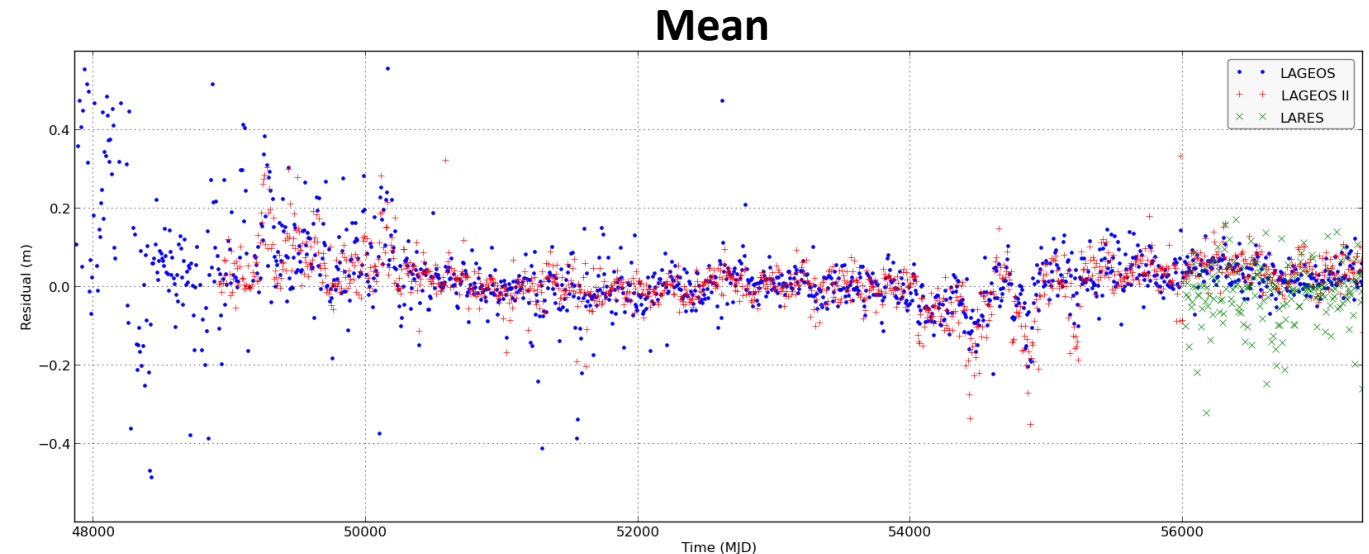
Range residuals: Root Mean Square (RMS) and Mean for the two LAGEOS satellites and LARES



Results on April 2016

In the case of LAGEOS we obtained a mean of about **2.2 cm** for the residuals and a RMS of about **1 cm**. In the case of LAGEOS II the residuals have a mean of about **1 cm** with a RMS of **0.9 cm**. Finally, for LARES residuals we obtained a mean value close to **-2 cm** with a RMS of about **1.7 cm**. Empirical accelerations have been estimated over an arc length of 7 days

LAGEOS (blue), LAGEOS II (red) and LARES (green). The starting epoch is MJD 47868 (December 8, 1989) for LAGEOS, MJD 48932 (November 13, 1992) for LAGEOS II and MJD 56023 (April 6, 2012) for LARES. The final epoch is December 25, 2015, for all three satellites

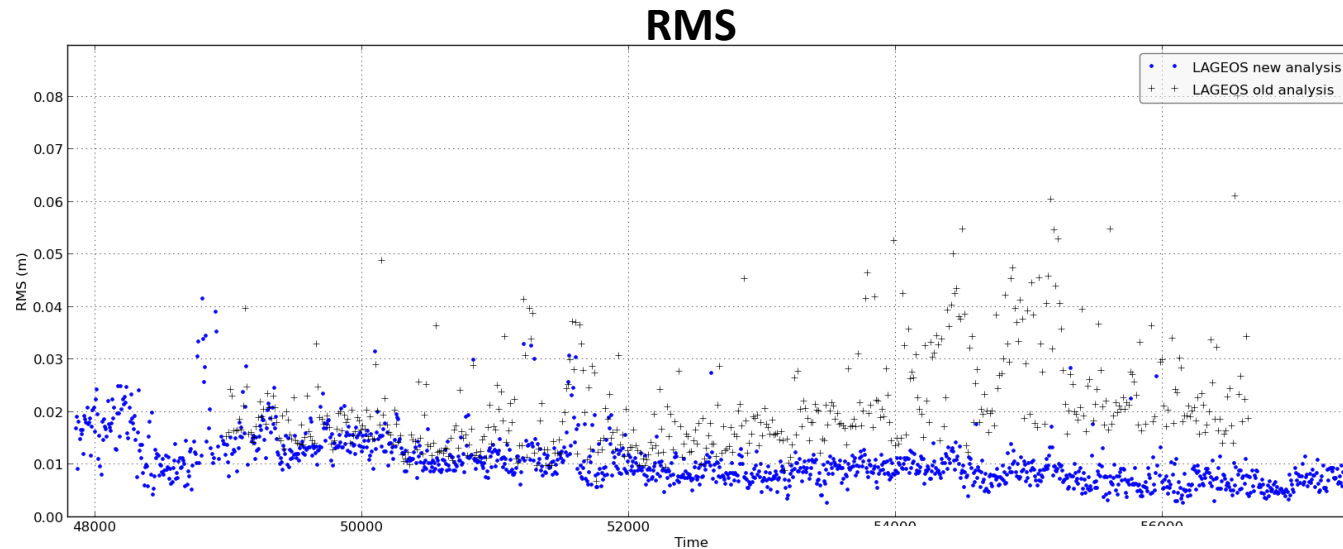


Precise Orbit Determination

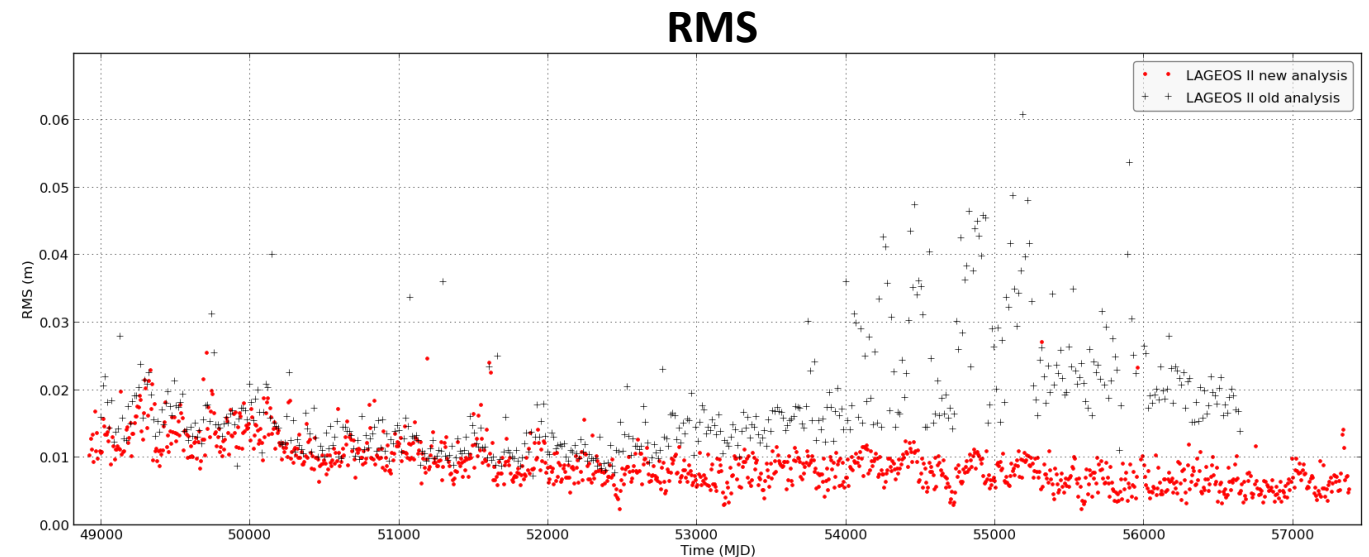
Root Mean Square (RMS) of the range residuals of the two LAGEOS satellites

Improvements with respect to 2015

Bottom: current (2016) best POD of LAGEOS II (red) compared with the best POD obtained in 2015 (black); the current mean RMS is about 0.9 cm vs 1.8 cm of previous analysis



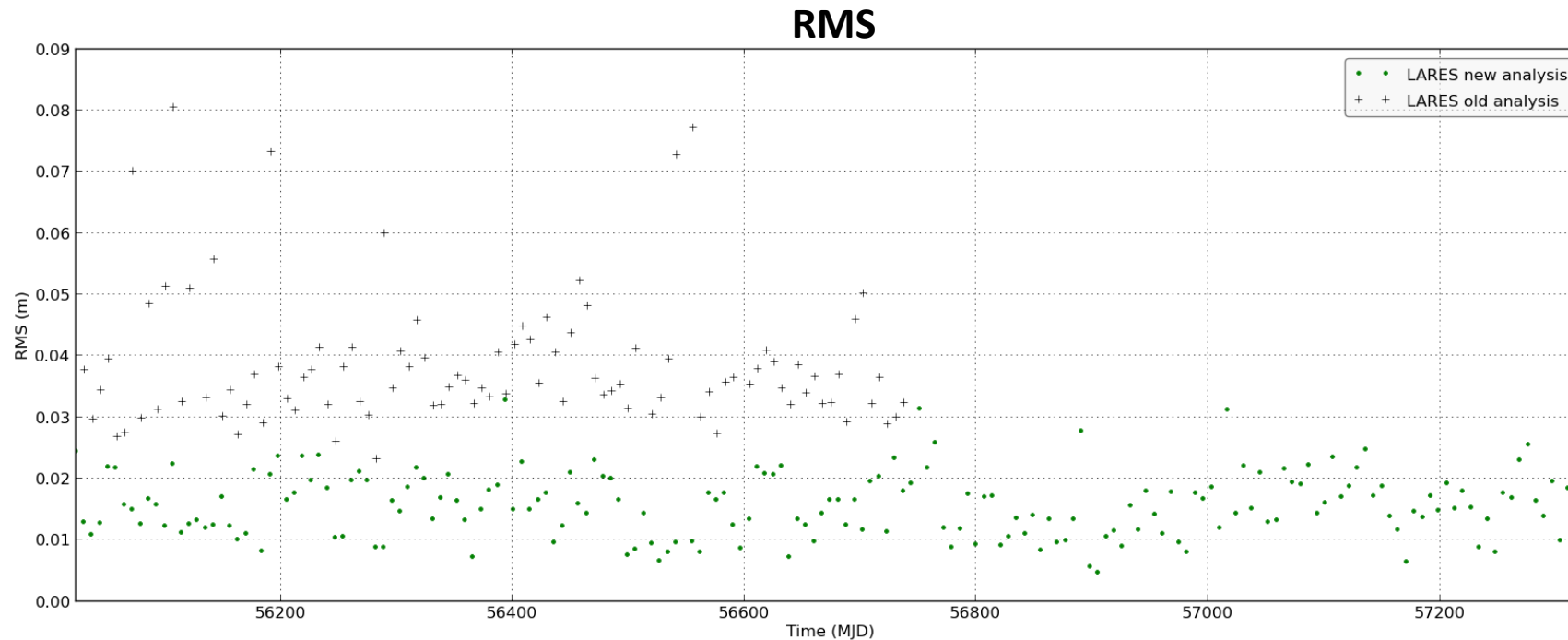
Top: current (2016) best POD of LAGEOS (blue) compared with the best POD obtained in 2015 (black); the current mean RMS is about 1 cm vs 2.1 cm of previous analysis



Precise Orbit Determination

Root Mean Square (RMS) of the range residuals of the LARES satellite

Improvements with respect to 2015



Current (2016) best POD of LARES (green) compared with the best POD obtained in 2015 (black); the current mean RMS is about 1.7 cm vs 3.7 cm of previous analysis

SPIN ON

Empirical accelerations have been not included in GEODYN II

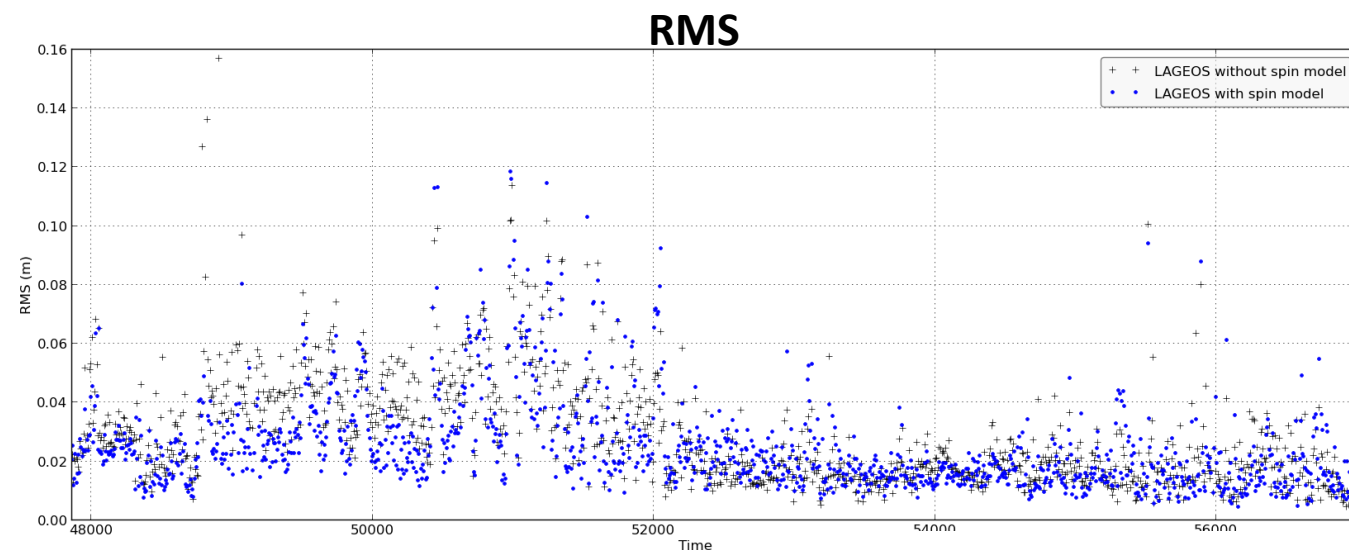
Precise Orbit Determination

Root Mean Square (RMS) of the range residuals of the two LAGEOS satellites

Further improvements when Spin is included in GEODYN II and the Earth-Yarkovsky effect is modelled

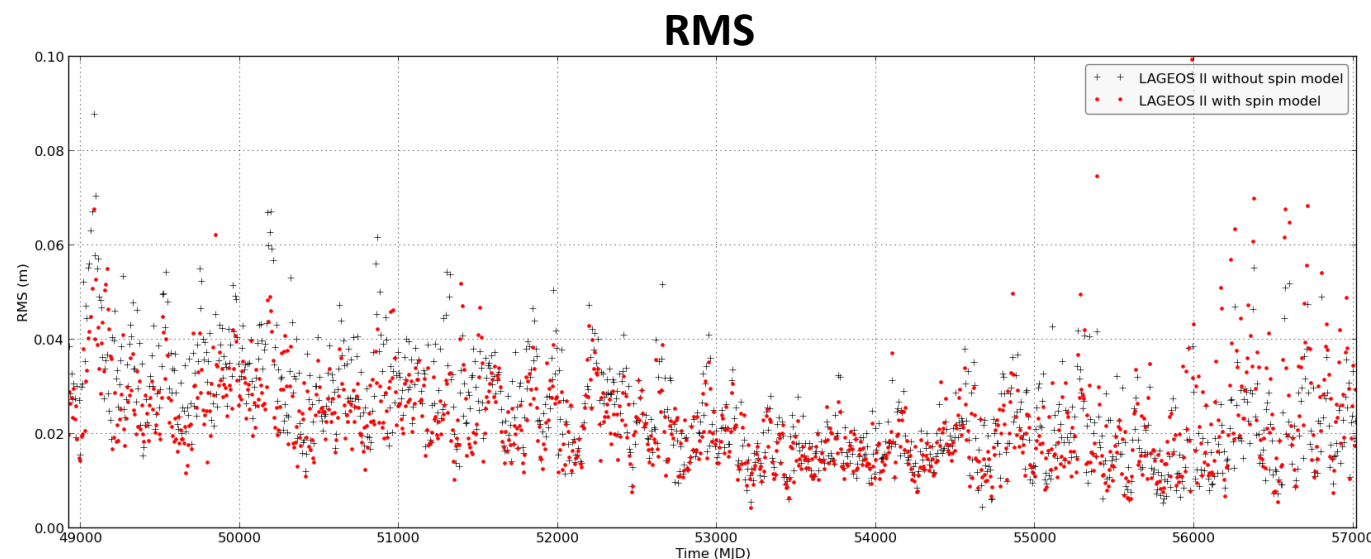
Bottom: In the case of LAGEOS II, the mean RMS is about 2.2 cm when modeling the Earth-Yarkovsky effect, compared to 2.5 cm when the thermal effect is not included in the GEODYN II setup

RMS: 2.5 cm → 2.2 cm



Top: in the case of LAGEOS the mean value of the RMS is close to 2.5 cm when modeling the Earth-Yarkovsky effect with the LARASE Spin Model, compared to 2.8 cm when the thermal effect is not included in the GEODYN II setup

RMS: 2.8 cm → 2.5 cm



Summary

- The LARASE experiment and its goals
- The internal structure of the two LAGEOS satellites
- The rotational dynamics and the Spin Model for the LAGEOS and LARES satellites
- Neutral drag effects on the LAGEOS and LARES satellites
- Solid and Ocean Tides on the LAGEOS and LARES satellites
- Precise Orbit Determination of the LAGEOS and LARES satellites
- Measurement of relativistic effects
- Conclusions and future work



Measurement of relativistic effects

Our main goals in the field of fundamental physics measurements fall in the following main targets:

- Schwarzschild precession (gravitoelectric field)
- Lense-Thirring precession (gravitomagnetic field)
- Geodetic (de Sitter) precession
- Post-Newtonian parameter (β , γ , α_1 , α_2 , ...)
- Constraints and limits to alternative theories of the gravitational interaction (Yukawa, non-symmetric/torsional ...)

We are now ready to start new refined measurements of the above relativistic effects with laser-ranged satellites. As said, there are two main aspects to satisfy:

1. obtain very precise measurements from the analysis of the post-fit residuals (after the POD)
2. provide a very reliable estimate of the systematics, i.e., accurate measurements

Measurement of relativistic effects

Gravito-electromagnetism: linearized theory of General Relativity (GR)

In the Weak-Field and Slow-Motion (**WFSM**) limit of the theory of **GR**, Einstein's equations reduce to a form quite similar to those of electromagnetism. Following this approach we have a:

- gravitoelectric field produced by masses, analogous to the electric field produced by charges
- gravitomagnetic field produced by mass currents, analogous to the magnetic field produced by electric currents.

$$G_{\alpha\beta} = 8\pi \frac{G}{c^4} T_{\alpha\beta}$$

$$\begin{cases} \bar{h}^{\alpha\beta}_{,\beta} = 0 \\ g_{\alpha\beta} = \eta_{\alpha\beta} + h_{\alpha\beta} \\ \Delta \bar{h}_{\alpha\beta} = 16\pi \frac{G}{c^4} T_{\alpha\beta} \end{cases}$$

$$\begin{cases} \bar{h}_{\alpha\beta} \equiv h_{\alpha\beta} - \frac{1}{2} \eta_{\alpha\beta} h \\ h \equiv h^\alpha_\alpha = \eta^{\alpha\beta} h_{\alpha\beta} \end{cases}$$

$$|h_{\alpha\beta}| \cong \left| \frac{\Phi}{c^2} \right| \leq 10^{-6}$$

$$\begin{cases} \bar{h}^{00} = 4 \frac{\Phi}{c^2} \\ \bar{h}^{0l} = -2 \frac{A^l}{c^2} \\ \bar{h}^{ij} = O(c^{-4}) \end{cases}$$

$$\Phi = -\frac{GM_\odot}{R_\odot}$$

$$A^l = \frac{G}{c} \frac{J^n x^k}{r^3} \varepsilon_{nk}^l$$

$$\eta_{\alpha\beta} = \begin{pmatrix} 1 & 0 & 0 & 0 \\ 0 & -1 & 0 & 0 \\ 0 & 0 & -1 & 0 \\ 0 & 0 & 0 & -1 \end{pmatrix}$$

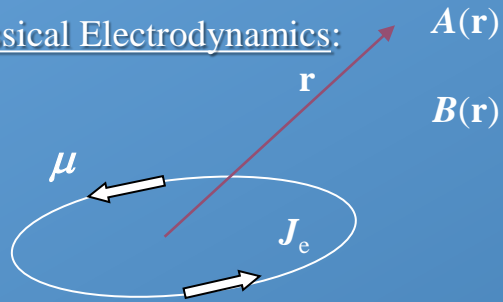
Gravitoelectric potential

Gravitomagnetic potential

Measurement of relativistic effects

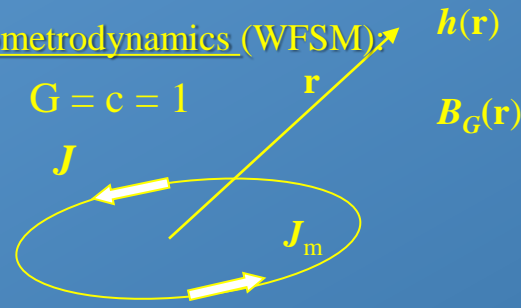
Formal analogy with electrodynamics: linearized theory of General Relativity (WFSM limit)

Classical Electrodynamics:



$$\Delta \vec{A} = -4\pi \cdot \vec{J}_e$$

Classical Geometrodynamics (WFSM)



$$\Delta \vec{h} = 16\pi \cdot \vec{J}_m$$

solution:

$$\vec{A}(\vec{r}) = \int \frac{\vec{J}_e(\vec{r}')}{|\vec{r} - \vec{r}'|} d^3r'$$

$$\vec{\mu} = \frac{1}{2} \int \vec{r} \wedge \vec{J}_e(\vec{r}) d^3r$$

$$\vec{A}(\vec{r}) \cong \frac{\vec{\mu} \wedge \vec{r}}{r^3}$$

$$\vec{B} = \vec{\nabla} \wedge \vec{A} \cong \frac{3\hat{r}(\hat{r} \cdot \vec{\mu}) - \vec{\mu}}{r^3}$$

$$\vec{F} = m \ddot{\vec{r}} = q(\vec{E} + \dot{\vec{r}} \wedge \vec{B})$$

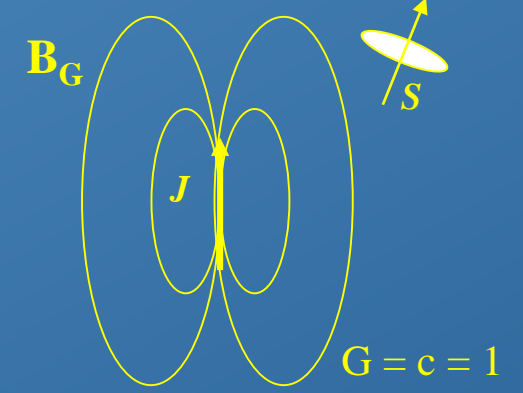
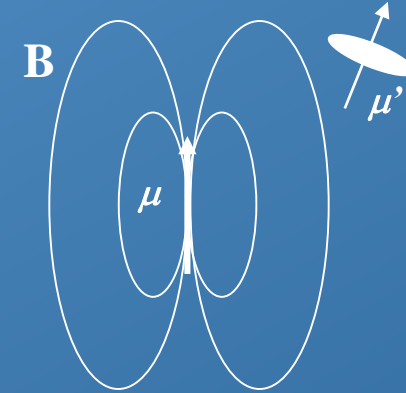
$$\vec{h}(\vec{r}) = -4 \int \frac{\vec{J}_m(\vec{r}')}{|\vec{r} - \vec{r}'|} d^3r'$$

$$\vec{J} = \int \vec{r} \wedge \vec{J}_m(\vec{r}) d^3r$$

$$\vec{h}(\vec{r}) \cong -2 \frac{\vec{J} \wedge \vec{r}}{r^3}$$

$$\vec{B}_G = \vec{\nabla} \wedge \vec{h} \cong -2 \frac{3\hat{r}(\hat{r} \cdot \vec{J}) - \vec{J}}{r^3}$$

$$\vec{F} = m \ddot{\vec{r}} = m \left(-\frac{M}{r^2} \hat{r} + \dot{\vec{r}} \wedge \vec{B}_G \right)$$



$$\vec{F} = (\vec{\mu}' \cdot \vec{\nabla}) \vec{B}$$

$$\vec{N} = \vec{\mu}' \wedge \vec{B}$$

$$\dot{\Omega} = -\dot{\vec{B}} = \frac{\vec{\mu} - 3\hat{r}(\hat{r} \cdot \vec{\mu})}{r^3}$$

$$\vec{F} = \frac{1}{2} (\vec{S} \cdot \vec{\nabla}) \vec{B}_G$$

$$\vec{N} = \frac{1}{2} \vec{S} \wedge \vec{B}_G$$

$$\dot{\Omega} = -\frac{1}{2} \dot{\vec{B}_G} = \frac{-\vec{J} + 3\hat{r}(\hat{r} \cdot \vec{J})}{r^3}$$

This phenomenon is known as dragging of gyroscopes or dragging of inertial frames

Therefore, mass currents (as the rotating Earth) drag gyroscopes and change the orientation of their axes

Measurement of relativistic effects

Gravitomagnetism

- Mass currents contribute to the curvature of spacetime
- Gravitomagnetism may be thought of as a manifestation of the way inertia originates in Einstein geometrodynamics ... “inertia here arises from mass there” ...
- The dragging of inertial frames or Lense-Thirring effect represents a weak manifestation (within GR) of Mach’s Principle (the experimental proof of the origin of local inertial forces, interpreted as gravitational forces)
- The full inclusion of Mach Principle in GR is still debated ...
- Anyway, the astrophysical and cosmological consequences are very significant ...

See “Gravitation and Inertia”, Ciufolini and Wheeler, 1995 for a deep insight into gravitomagnetism

Measurement of relativistic effects

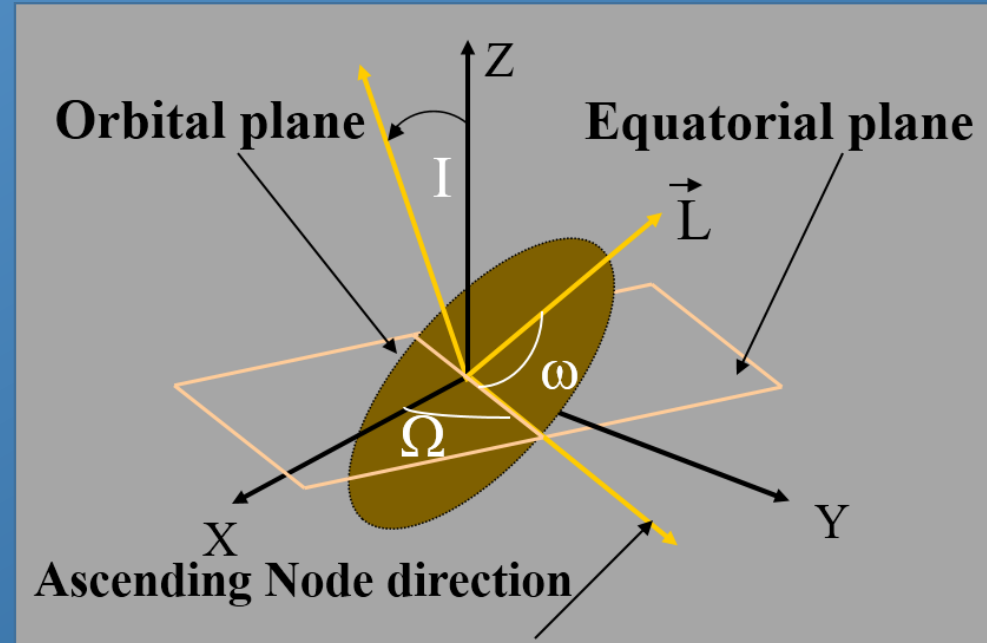
Gravitomagnetism: orbit precession

Lense-Thirring, Phys. Z, 19, 1918

$$\dot{\Omega}_{LT} = \mu \frac{2G}{c^2 a^3} \frac{J_{\oplus}}{(1 - e^2)^{3/2}}$$

$$\dot{\omega}_{LT} = -\mu \frac{6G}{c^2 a^3} \frac{J_{\oplus}}{(1 - e^2)^{3/2}} \cos I$$

$$\mu \neq \frac{1 + \gamma}{2}$$

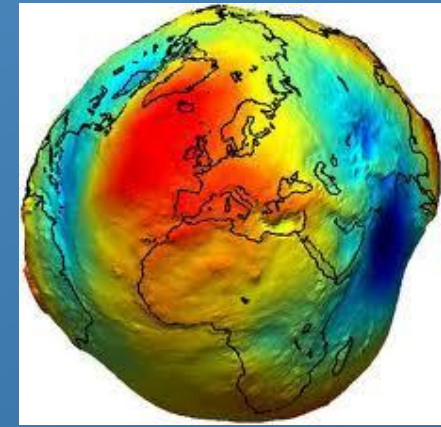


mas/yr	LAGEOS	LAGEOS II	LARES
$\dot{\Omega}_{LT}$	30.7	31.5	118.5
$\dot{\omega}_{LT}$	31.3	- 57.3	- 215.6

30 mas/yr at LAGEOS altitude ($\cong 5900$ km) corresponds to a displacement of about 1.8 m/yr!

Measurement of relativistic effects

Big problem with the **even zonal** harmonics uncertainties: **systematic errors**



$$V(r, \varphi, \lambda) = -\frac{GM_{\oplus}}{r} \left[1 + \sum_{\ell=2}^{\infty} \sum_{m=0}^{\ell} \left(\frac{R_{\oplus}}{r} \right)^{\ell} P_{\ell m}(\sin \varphi) (C_{\ell m} \cos m\lambda + S_{\ell m} \sin m\lambda) \right]$$

Spherical harmonics
development of the Earth's
potential $V(r)$



$m = 0$ → zonal harmonics

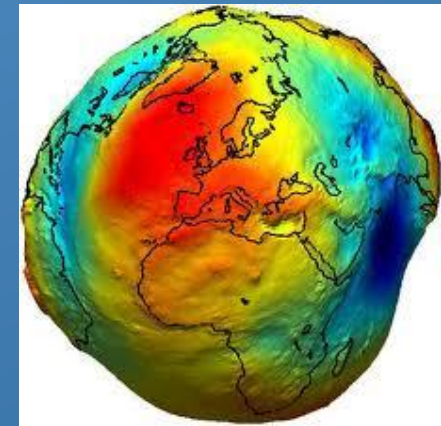
$$V(r) = -\frac{GM_{\oplus}}{r} \left[1 - J_2 \left(\frac{R_{\oplus}}{r} \right)^2 \frac{3\cos^2\vartheta - 1}{2} + \dots \right]$$

Dependency from the even zonal harmonics
only, their uncertainties mimics a secular
effect in the right ascension of the node and
also in the argument of pericenter

$$\dot{\Omega}_{class} = -\frac{3}{2}n \left(\frac{R_{\oplus}}{a} \right)^2 \frac{\cos i}{(1 - e^2)^2} \delta J_2 + \dots$$

Measurement of relativistic effects

Big problem with the **even zonal** harmonics uncertainties: **systematic errors**



$$V(r, \varphi, \lambda) = -\frac{GM_{\oplus}}{r} \left[1 + \sum_{\ell=2}^{\infty} \sum_{m=0}^{\ell} \left(\frac{R_{\oplus}}{r} \right)^{\ell} P_{\ell m}(\sin \varphi) (C_{\ell m} \cos m\lambda + S_{\ell m} \sin m\lambda) \right]$$

Spherical harmonics
development of the Earth's
potential $V(r)$



$m = 0$ → zonal harmonics

$$V(r) = -\frac{GM_{\oplus}}{r} \left[1 - J_2 \left(\frac{R_{\oplus}}{r} \right)^2 \frac{3\cos^2\vartheta - 1}{2} + \dots \right]$$

Dependency from the even zonal harmonics
only, their uncertainties mimics a secular
effect in the right ascension of the node and
argument of pericenter

$$\dot{\Omega}^{Class} \cong -\frac{3}{2}n \left(\frac{R_{\oplus}}{a} \right)^2 \frac{\cos I}{(1-e^2)^2} \left\{ J_2 + J_4 \left[\frac{5}{8} \left(\frac{R_{\oplus}}{a} \right)^2 (7\sin^2 I - 4) \frac{(1 + \frac{3}{2}e^2)}{(1-e^2)^2} \right] + \dots \right\}$$

$$\dot{\omega}^{Class} \cong -\frac{3}{4}n \left(\frac{R_{\oplus}}{a} \right)^2 \frac{(1 - 5\cos^2 I)}{(1-e^2)^2} \left\{ J_2 + J_4 \left[\frac{5}{256} \left(\frac{R_{\oplus}}{a} \right)^2 (7\sin^2 I - 4) \frac{C(e, I)}{(1 - 5\cos^2 I)} \right] + \dots \right\}$$



Measurement of relativistic effects

Big problem with the **even zonal** harmonics uncertainties: **systematic errors**

We have two main unknowns:

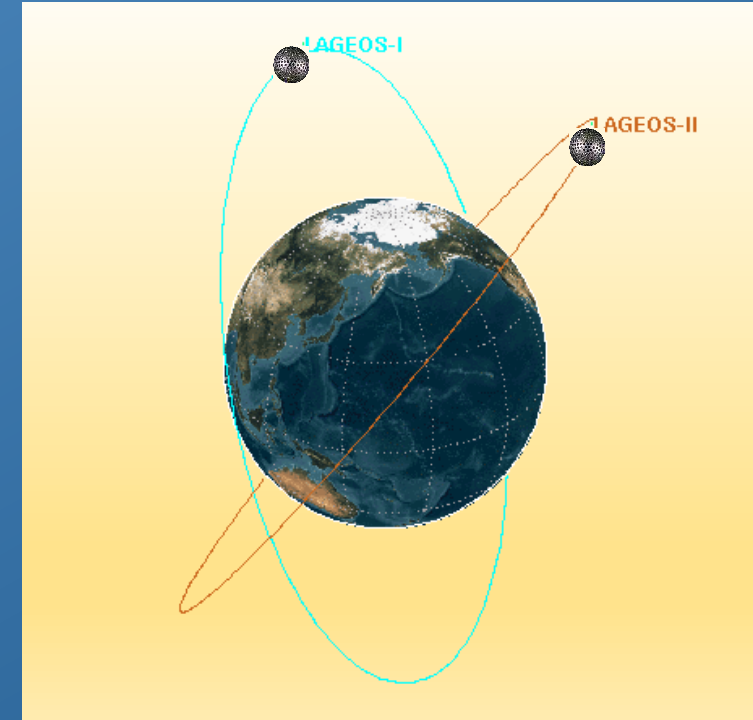
1. the precession on the node due to the LT effect: μ_{LT} ;
2. the J_2 uncertainty: δJ_2 ;

Hence, we need two observables in such a way to eliminate the uncertainty of the first even zonal harmonic and solve for the LT effect. These observables are:

1. LAGEOS node: $\delta\Omega_{Lageos}$;
2. LAGEOS II node: $\delta\Omega_{LageosII}$;

$\mu = \delta\dot{\Omega}_I^{res} + k\delta\dot{\Omega}_{II}^{res}$ represents the solution of a system of two equations in two unknowns

Of course, including the pericenter, we have three observables: LAGEOS II perigee has been considered thanks to its larger eccentricity ($\cong 0.014$) with respect to that of LAGEOS ($\cong 0.004$)



Measurement of relativistic effects

LARASE measurements of relativistic precessions:

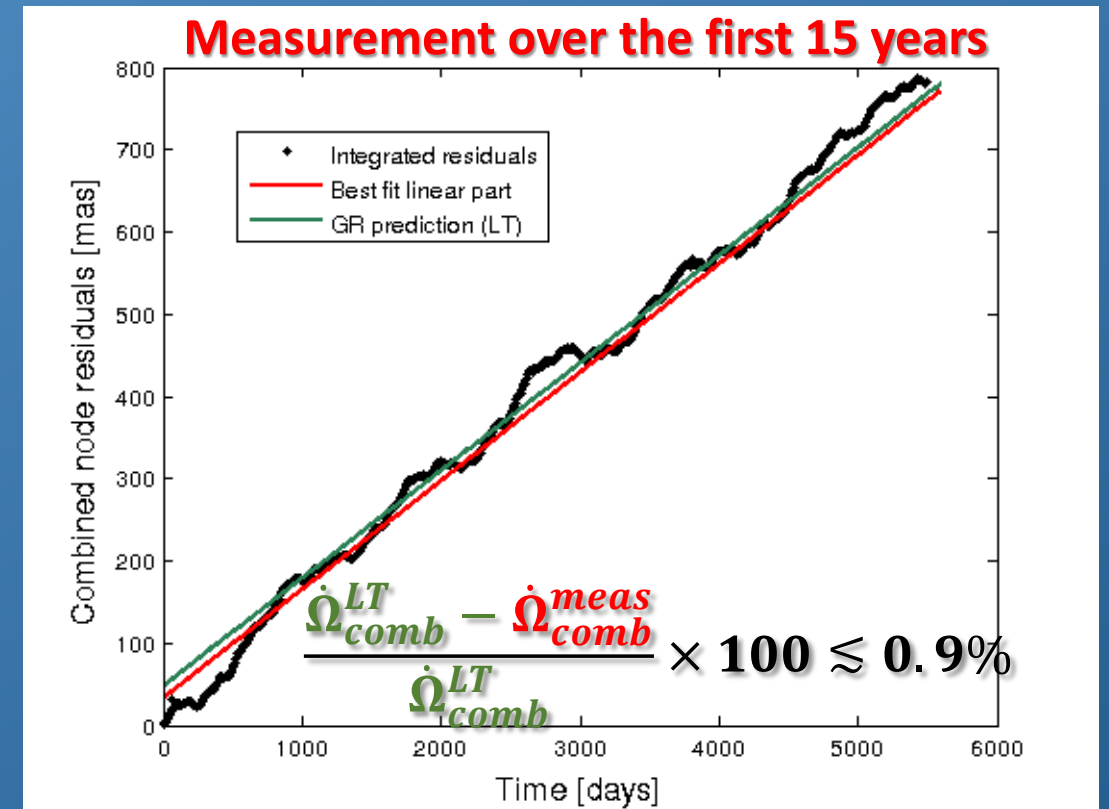
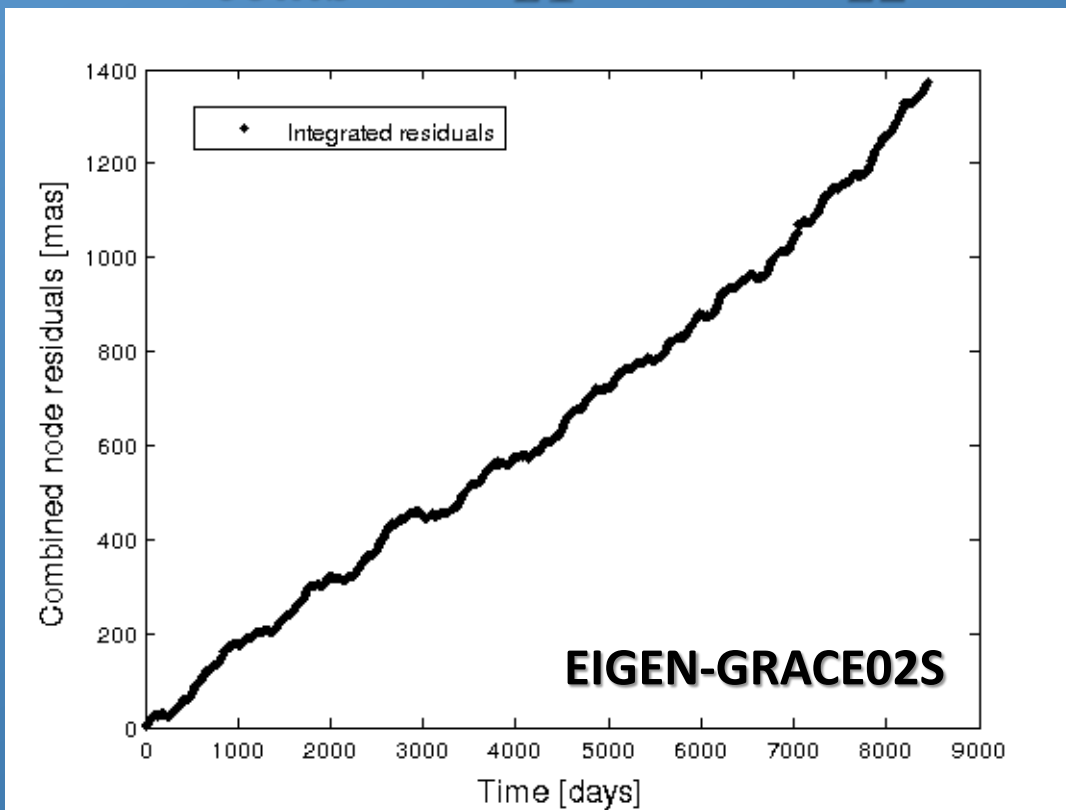
1. A new preliminary measurement of the Lense-Thirring precession with the two LAGEOS satellites (2016)
2. A new preliminary measurement of the Lense-Thirring precession with the two LAGEOS satellites and LARES (2016)
3. Measurement of the overall GR precession of LAGEOS II pericenter (2014)
4. Constraints on alternative theories of gravitation (2014)

Measurement of relativistic effects

A preliminary new measurement of the Lense-Thirring effect with the two LAGEOS only

This is a 23.6 years data analysis of the orbit of the two LAGEOS only:

$$\dot{\Omega}_{comb} = \dot{\Omega}_{L1}^{res} + k \cdot \dot{\Omega}_{L2}^{res}$$

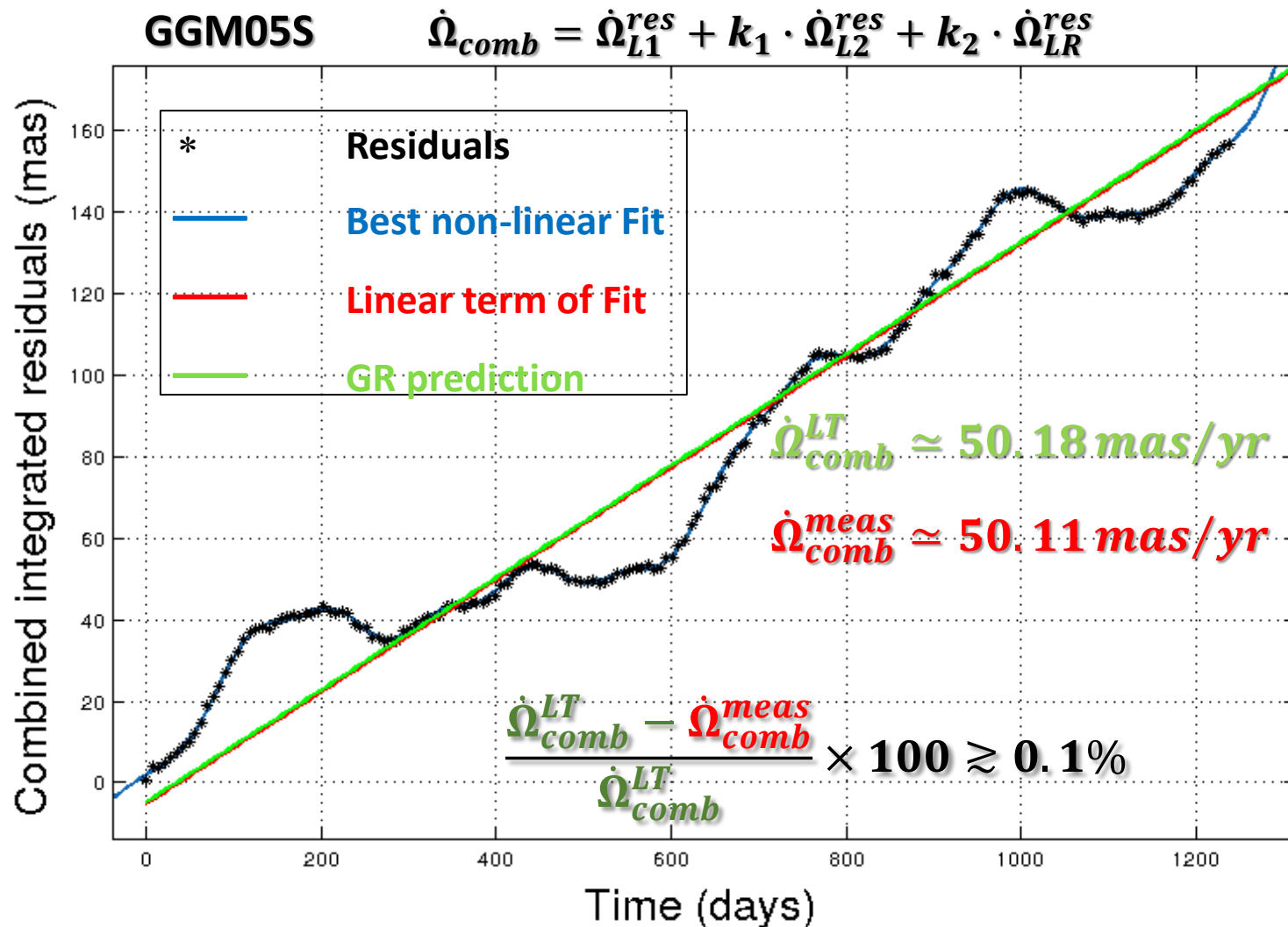


To be compared with Ciufolini and Pavlis (2004) that, after a dedicated analysis over 11 years, obtained:

$$\frac{\Omega_{comb}^{LT} - \Omega_{comb}^{meas}}{\Omega_{comb}^{LT}} \times 100 \gtrsim 0.6\%$$

Measurement of relativistic effects

A very preliminary new measurement of the Lense-Thirring effect with the two LAGEOS and LARES (3.4 yr)



We fitted also for a minimum of three to a maximum of twelve tidal waves (both solid and ocean):

$$\Omega^{Fit} = a + b \cdot t + \sum_{i=1}^n A_i \cdot \sin\left(\frac{2\pi}{P_i} \cdot t + \Phi_i\right)$$

Indeed, tides mismodelling plus unmodelled nongravitational forces due to thermal effects may corrupt the measurement of the relativistic effect.

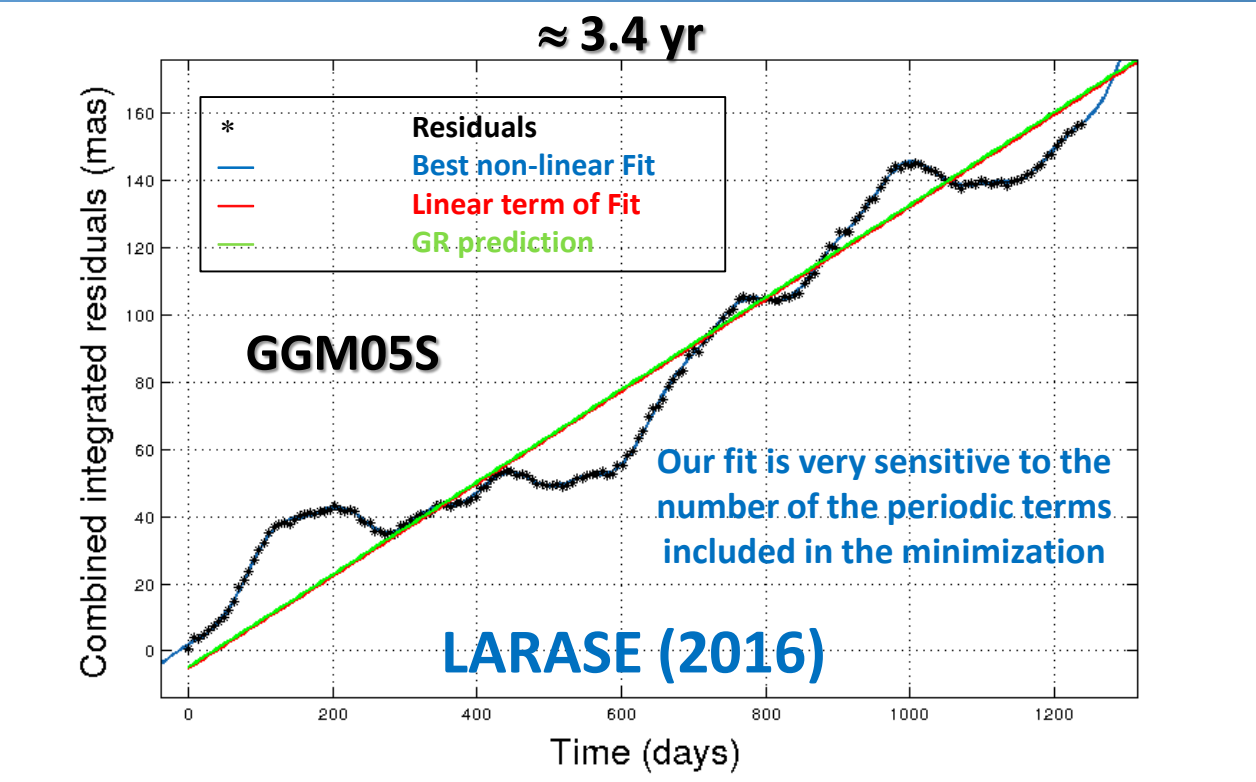
For instance, the (both solid and ocean) **K1** tides have the same periods of the right ascension of the node of the satellites:

≈ 1044 days, ≈ 569 days and ≈ 224 days

$$\dot{\Omega}_{comb} = \dot{\Omega}_{L1}^{res} + k_1 \cdot \dot{\Omega}_{L2}^{res} + k_2 \cdot \dot{\Omega}_{LR}^{res}$$

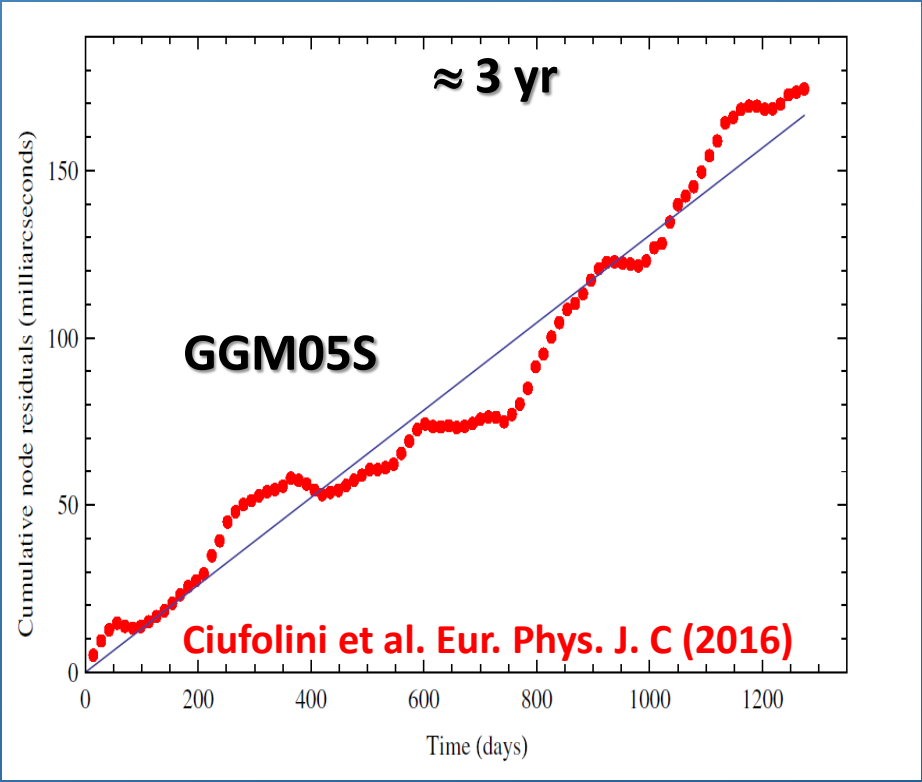
Measurement of relativistic effects

Comparison with a recent measurement



$$\mu = (0.999 \pm \varepsilon(\text{fit})) \pm \varepsilon(\text{sys})$$

Up to 9% from a sensitivity analysis of the main tidal waves



$$\mu = (0.994 \pm 0.002) \pm 0.05$$

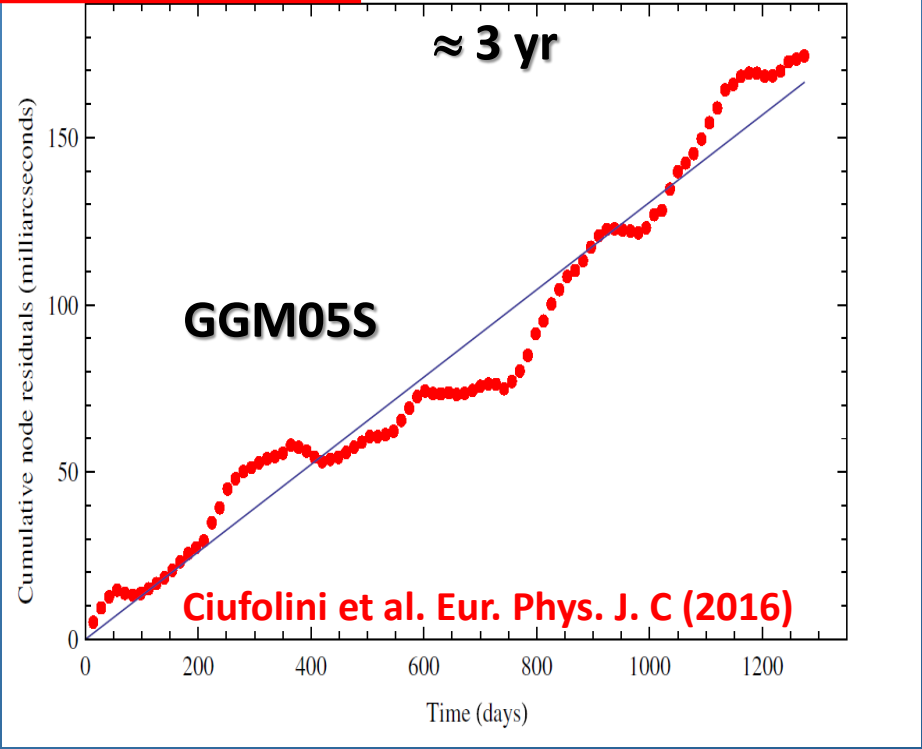
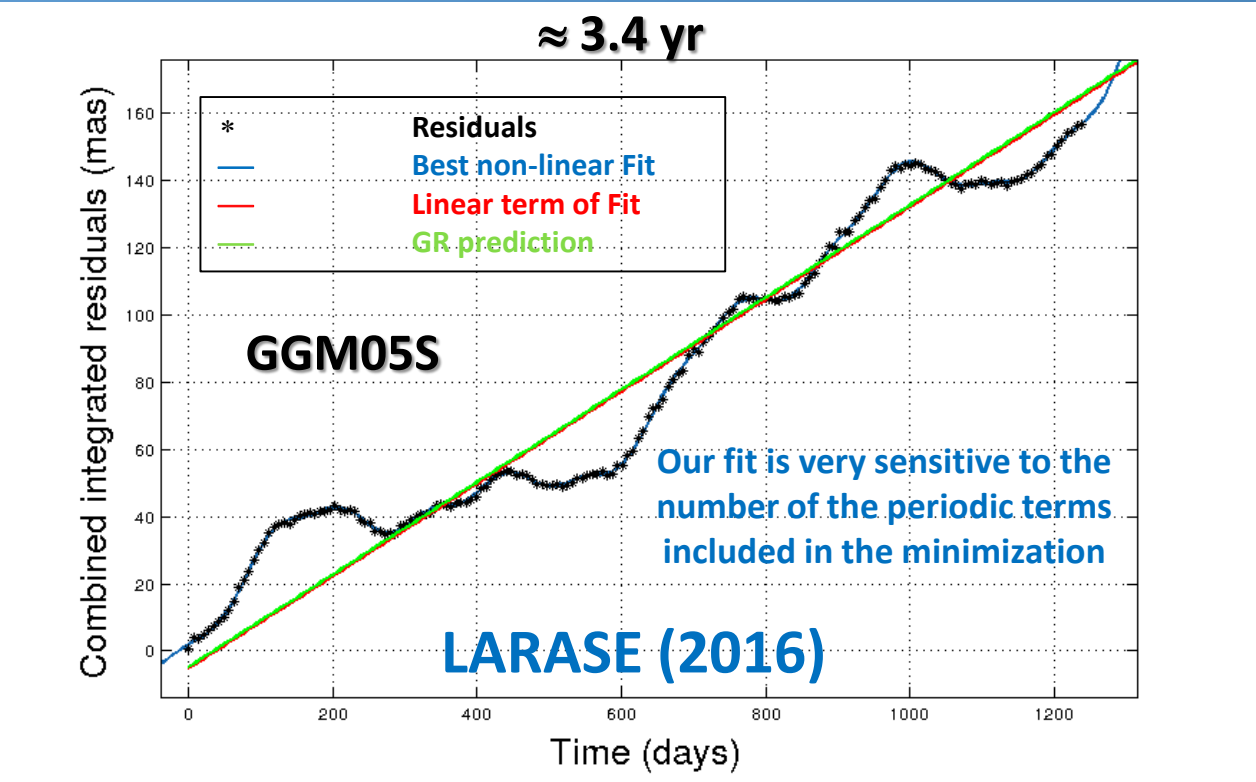
0.2% formal error of the fit (1-sigma) plus 5% preliminary estimate of systematics (4% grav. + 1% non-grav.)

$$\dot{\Omega}_{comb} = \dot{\Omega}_{L1}^{res} + k_1 \cdot \dot{\Omega}_{L2}^{res} + k_2 \cdot \dot{\Omega}_{LR}^{res}$$

Measurement of relativistic effects

Comparison with a recent measurement

Indeed, a robust and reliable estimate of systematics is one of the primary goals of LARASE !



$$\mu = (0.999 \pm \varepsilon(fit)) \pm \varepsilon(sys)$$

$$\mu = (0.994 \pm 0.002) \pm 0.05$$

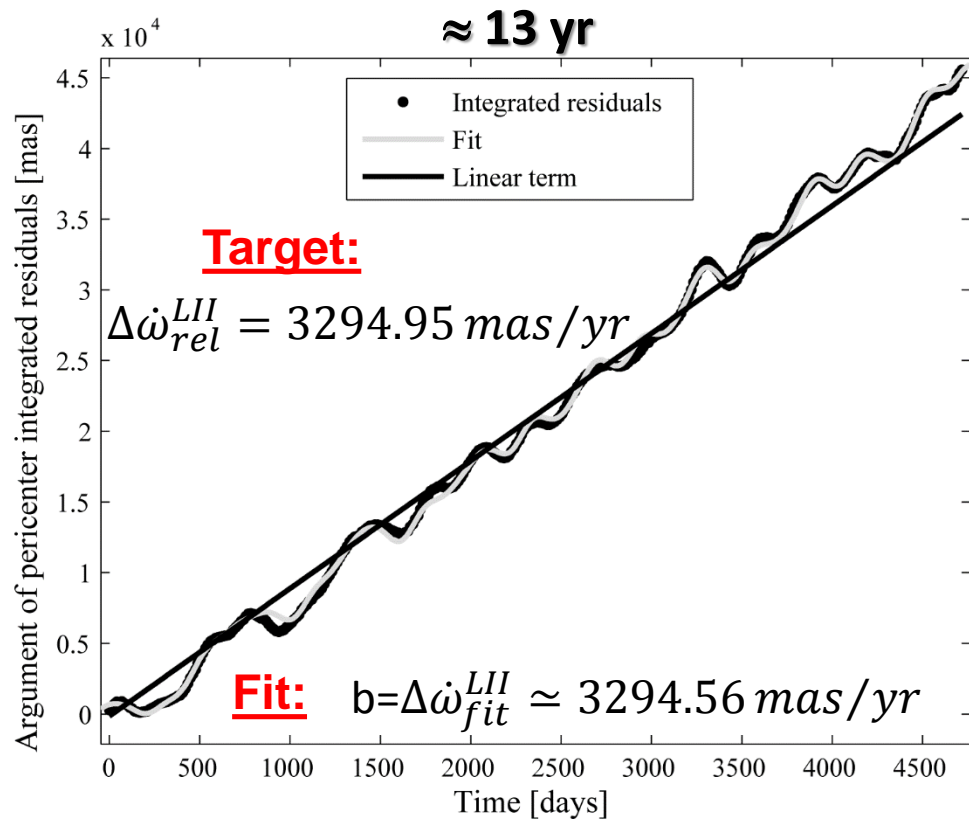
Up to 9% from a sensitivity analysis of the main tidal waves

0.2% formal error of the fit (1-sigma) plus 5% preliminary estimate of systematics (4% grav. + 1% non-grav.)

Measurement of relativistic effects

A precise and accurate measurement performed in the recent pass (2014):

Fit to the pericenter residuals of LAGEOS II



Lucchesi, Peron, *Phy. Rev. D*, 89, 2014

Fitting function for the pericenter:

$$\Delta\omega^{FIT} = a + b \cdot t + c(t - t_0)^2 + \sum_{i=1}^n D_i \sin\left(\frac{2 \cdot \pi}{P_i} \cdot t + \Phi_i\right)$$

- We obtained $b \simeq 3294.6 \text{ mas/yr}$, very close to the prediction of **GR**
- The discrepancy is just **0.01%**
- From a sensitivity analysis, with constraints on some of the parameters that enter into the least squares fit, we obtained an upper bound of **0.2%**

$$\Delta\dot{\omega} = \Delta\dot{\omega}_{GP} + \Delta\dot{\omega}_{NGP} + \varepsilon \cdot \Delta\dot{\omega}_{GR}$$

$$\varepsilon = 1 - (0.12 \pm 2.10) \cdot 10^{-3} \pm 2.5 \cdot 10^{-2}$$

Measurement of relativistic effects

Lucchesi, Peron, *Phy. Rev. D*, 89, 2014

Summary of the constraints in gravitational theories so far obtained

TABLE XVIII. Summary of the results obtained in the present work; together with the measurement error budget, the constraints on fundamental physics are listed and compared with the literature.

Parameter	Values and uncertainties (this study)	Uncertainties (literature)	Remarks
$\epsilon_\omega - 1$	$-1.2 \times 10^{-4} \pm 2.10 \times 10^{-3} \pm 2.54 \times 10^{-2}$...	Error budget of the perigee precession measurement in the field of the Earth
$\frac{ 2+2\gamma-\beta }{3} - 1$	$-1.2 \times 10^{-4} \pm 2.10 \times 10^{-3} \pm 2.54 \times 10^{-2}$	$\pm(1.0 \times 10^{-3}) \pm (2 \times 10^{-2})^a$	Constraint on the combination of PPN parameters
$ \alpha $	$\lesssim 0.5 \pm 8.0 \pm 101 \times 10^{-12}$	$\pm 1 \times 10^{-8b}$	Constraint on a possible (Yukawa-like) NLRI
$\mathcal{C}_{\oplus \text{LAGEOSII}}$	$\leq (0.003 \text{ km})^4 \pm (0.036 \text{ km})^4 \pm (0.092 \text{ km})^4$	$\pm(0.16 \text{ km})^{4c}; \pm(0.087 \text{ km})^{4d}$	Constraint on a possible NSGT
$ 2t_2 + t_3 $	$\lesssim 3.5 \times 10^{-4} \pm 6.2 \times 10^{-3} \pm 7.49 \times 10^{-2}$	3×10^{-3e}	Constraint on torsion

^aFrom the preliminary estimate of the systematic errors of [166] for the perihelion precession of Mercury.

^bFrom [167] with Lunar-LAGEOS *GM* measurements.

^cFrom [5] and based on a partial estimate for the systematic errors.

^dFrom [7] and based on the analysis of the systematic errors only.

^eFrom [168] with no estimate for the systematic errors.

Measurement of relativistic effects

Lucchesi, Peron, *Phy. Rev. D*, 89, 2014

Summary of the constraints in gravitational theories so far obtained

TABLE XVIII. Summary of the results obtained in the present work; together with the measurement error budget, the constraints on fundamental physics are listed and compared with the literature.

Parameter	Values and uncertainties (this study)	Uncertainties (literature)	Remarks
$\epsilon_\omega - 1$	$-1.2 \times 10^{-4} \pm 2.10 \times 10^{-3} \pm 2.54 \times 10^{-2}$...	Error budget of the perigee precession measurement in the field of the Earth
$\frac{ 2+2\gamma-\beta }{3} - 1$	$-1.2 \times 10^{-4} \pm 2.10 \times 10^{-3} \pm 2.54 \times 10^{-2}$	$\pm(1.0 \times 10^{-3}) \pm (2 \times 10^{-2})^a$	Constraint on the combination of PPN parameters
$ \alpha $	$\lesssim 0.5 \pm 8.0 \pm 101 \times 10^{-12}$	$\pm 1 \times 10^{-8b}$	Constraint on a possible (Yukawa-like) NLRI
$\mathcal{C}_{\oplus \text{LAGEOS II}}$	$\leq (0.003 \text{ km})^4 \pm (0.036 \text{ km})^4 \pm (0.092 \text{ km})^4$	$\pm(0.16 \text{ km})^{4c}; \pm(0.087 \text{ km})^{4d}$	Constraint on a possible NSGT
$ 2t_2 + t_3 $	$\lesssim 3.5 \times 10^{-4} \pm 6.2 \times 10^{-3} \pm 7.49 \times 10^{-2}$	3×10^{-3e}	Constraint on torsion

^aFrom the preliminary estimate of the systematic errors of [166] for the perihelion precession of Mercury.

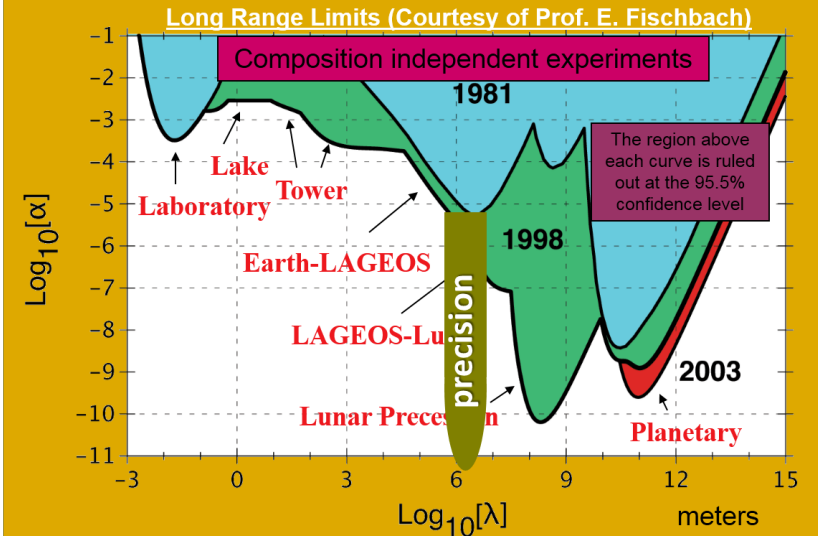
^bFrom [167] with Lunar-LAGEOS *GM* measurements.

^cFrom [5] and based on a partial estimate for the systematic errors.

^dFrom [7] and based on the analysis of the systematic errors only.

^eFrom [168] with no estimate for the systematic errors.

Constraints on a long-range force: Yukawa-like interaction



Reference: Coy, Fischbach, Hellings, Standish, & Talmadge (2003)

Conclusions and future work

The **LARASE** (**LA**ser **RA**nged **S**atellites **E**xperiment) activities, in terms of orbit modelling improvements and relativistic measurements, are ongoing:

- We have started an important activity aiming to improve the dynamical models of the LAGEOS and LARES satellites, especially with regard to the non-gravitational perturbations, with significant results for the:
 - Spin evolution
 - Neutral drag
- POD set up (stations position/velocity and biases, International Conventions/Reference frames, etc.) is in line with that of the Analysis Centers of the ILRS
- POD is very good for the two LAGEOS and some improvement is still expected for LARES
- The preliminary measurements of relativistic effects are very promising
- A new study has been started in order to improve the thermal models of the two LAGEOS and to develop a thermal model for LARES (but see Nguyen and Matzner (2015) for a first significant study in this direction: Eur. Phys. J. Plus 130, 206)

Testing the gravitational interaction in the field of the Earth via satellite laser ranging and the Laser Ranged Satellites Experiment (LARASE)

D M Lucchesi^{1,2,3}, L Anselmo², M Bassan^{3,4}, C Pardini²,
R Peron^{1,3}, G Pucacco^{3,4} and M Visco^{1,3}

¹ Istituto di Astrofisica e Planetologia Spaziali (IAPS/INAF), Via del Fosso del Cavaliere 100, I-00133 Roma, Italy

² Istituto di Scienza e Tecnologie della Informazione (ISTI/CNR), Via G. Moruzzi 1, I-56124 Pisa, Italy

³ Istituto Nazionale di Fisica Nucleare (INFN), Sezione di Roma Tor Vergata, Via della Ricerca Scientifica 1, I-00133 Roma, Italy

⁴ Dipartimento di Fisica, Università di Roma Tor Vergata, Via della Ricerca Scientifica 1, I-00133 Roma, Italy

E-mail: david.lucchesi@iaps.inaf.it

Received 24 March 2015, revised 1 June 2015

Accepted for publication 15 June 2015

Published 14 July 2015



CrossMark

The LARASE experiment and its goals

LARES a new laser ranged satellite:

On February 13th 2012 **LARES** (ASI) was successfully launched in its orbit with the qualification flight of the VEGA launcher of the European Space Agency (ESA)

CC BY 3.0



LAser **RElativity **S**atellite**



Principal Investigator:
Ciufolini I. (Univ. Lecce)

Main objective:
Measurement of the Lense–Thirring
effect @ 1%

LARES has been obtained by working a single piece of tungsten alloy of high density (18000 kg/m^3)

The LARASE experiment and its goals

- SLR measurements from more than 50 stations, plus;
- appropriate techniques of data analysis and processing, allow us to separate:
 1. Earth rotation;
 2. station movements with respect to the geocenter;
 3. satellite orbit;
- Then, from the analysis of the satellite orbital perturbations we can derive:
 - A. Earth gravity field harmonic coefficients;
 - B. tidal parameters (both solid and ocean tides);
 - C. exchange of angular momentum between Earth crust and atmosphere;
 - D. mantle structure;
 - E. post-glacial rebound effects;
 - F. dynamic effects of Geometrodynamics;

The LARASE experiment and its goals

- Dynamic effects of Geometrodynamics:

Today, the relativistic corrections (both of Special and General relativity) are an essential aspect of (dirty) Celestial Mechanics as well as of the electromagnetic propagation in space:

- these corrections are included in the orbit determination and analysis software for Earth's satellites and interplanetary probes;
- these corrections are necessary for spacecraft navigation and GPS satellites;
- these corrections are necessary for refined studies in the field of geodesy and geodynamics;

Thermal Thrust perturbations: the solar Yarkovsky–Schach effect

The main Thermal Thrust perturbations are due to the:

- Sun visible radiation when modulated by the satellite eclipses: Yarkovsky–Schach effect
 - Earth's infrared radiation: Earth–Yarkovsky (Rubincam effect)
- Unmodelled Thermal Thrust perturbations deeply impact on the orbit of a satellite with long-period effects in several orbital elements
- They are function of the spin-vector behaviour

The long-period effects arising from the Yarkovsky–Schach effect are particularly effective on:

- semi-major axis, eccentricity, argument of perigee and eccentricity vector excitations
- and they limit the precision and accuracy of relativistic measurements

Thermal Thrust perturbations: the solar Yarkovsky–Schach effect

Rapid spin approximation:

- the disturbing acceleration has only a component along the rotation axis

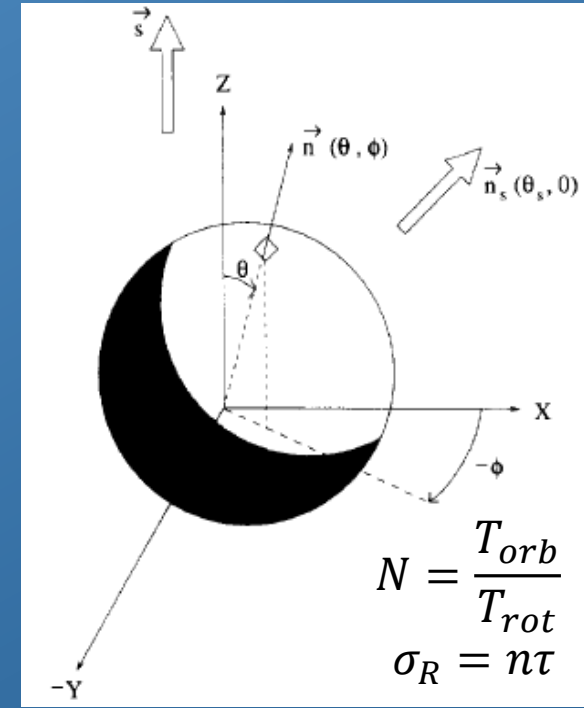
$$\vec{a}_z = \frac{16}{9} \pi R^2 \frac{\varepsilon \sigma}{mc} T_0^3 \Delta T \cos \vartheta_s \Gamma_z(\lambda) \hat{z}$$

General spin:

- the disturbing acceleration has in addition also two equatorial components

$$\vec{a}_x = \frac{16}{9} \pi R^2 \frac{\varepsilon \sigma}{mc} T_0^3 \Delta T \sin \vartheta_s \frac{\Gamma_x(\lambda, N)}{1 + N^2 \sigma_R^2} \hat{x}$$

$$\vec{a}_y = \frac{16}{9} \pi R^2 \frac{\varepsilon \sigma}{mc} T_0^3 \Delta T \sin \vartheta_s \frac{\Gamma_y(\lambda, N)}{1 + N^2 \sigma_R^2} \hat{y}$$



The ratios among the involved characteristic times are very important in defining the approximation:

- CCRs thermal inertia τ
- Rotational period T_{rot}
- Orbital period T_{orb}

Thermal Thrust perturbations: the solar Yarkovsky–Schach effect

LARASE activities: the general model for the Yarkovsky–Shach effect

Following the original work of Farinella and Vokrouhlicky (PSS, 44, 12, 1996) on LAGEOS, — and on the basis of the simplified model of Afonso et al. (Ann. Geophys. 7, 1989) — we completed and extended their generalization of the perturbing acceleration due to the Yarkovsky–Schach effect from the rapid spin case to the slowly rotating case, i.e. to the general case.

In particular, we:

- completed the generalization to all LAGEOS's orbital elements
- applied the generalization to LAGEOS II and to all its orbital elements
- started to compare the results with the satellites orbital residuals

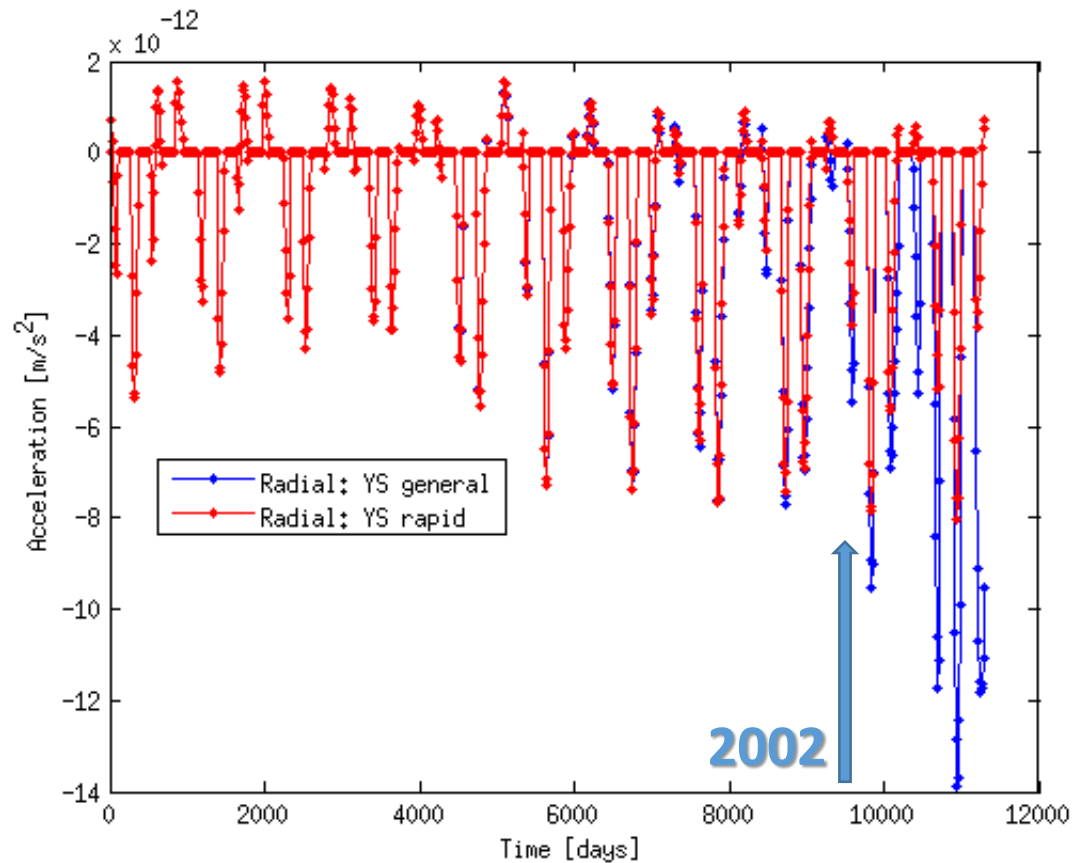
We plan to extend this generalization also to the Earth–Yarkovsky effect as soon as possible

Thermal Thrust perturbations: the solar Yarkovsky–Schach effect

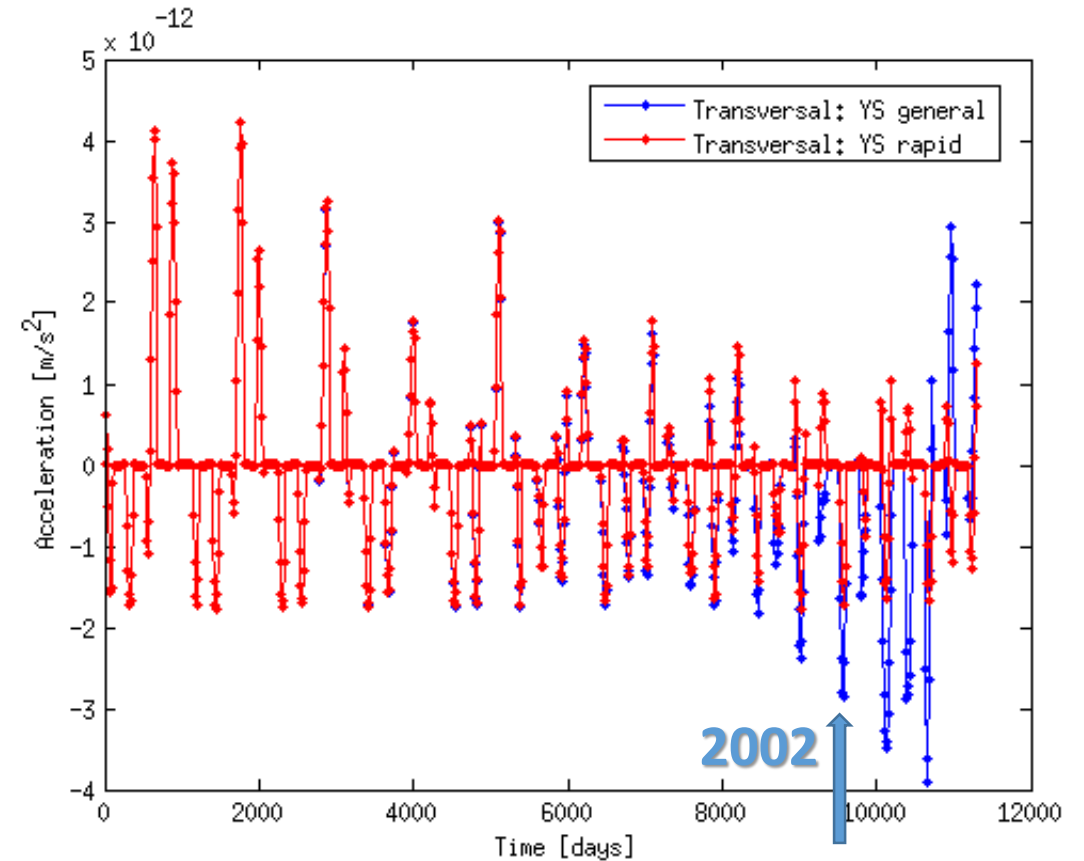
LARASE activities: comparison between the two models in the case of LAGEOS

Starting epoch, May 1976

Radial [R]



Transversal [T]

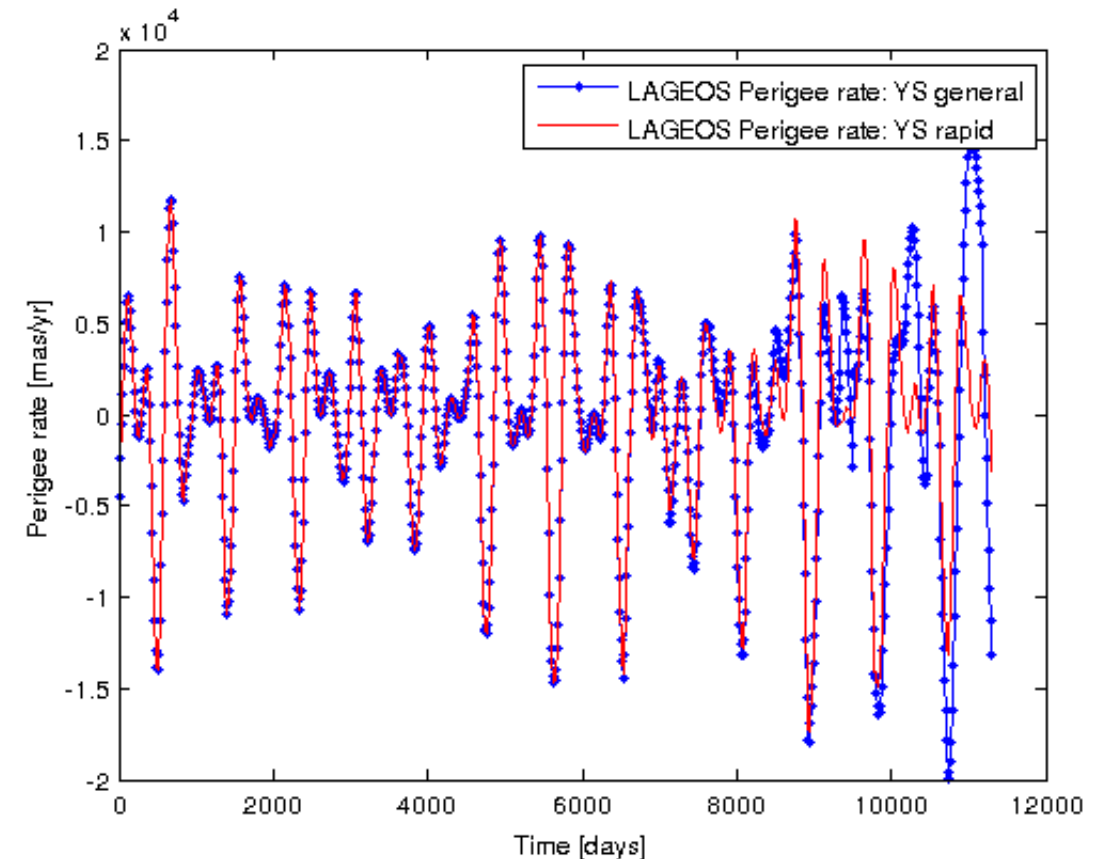
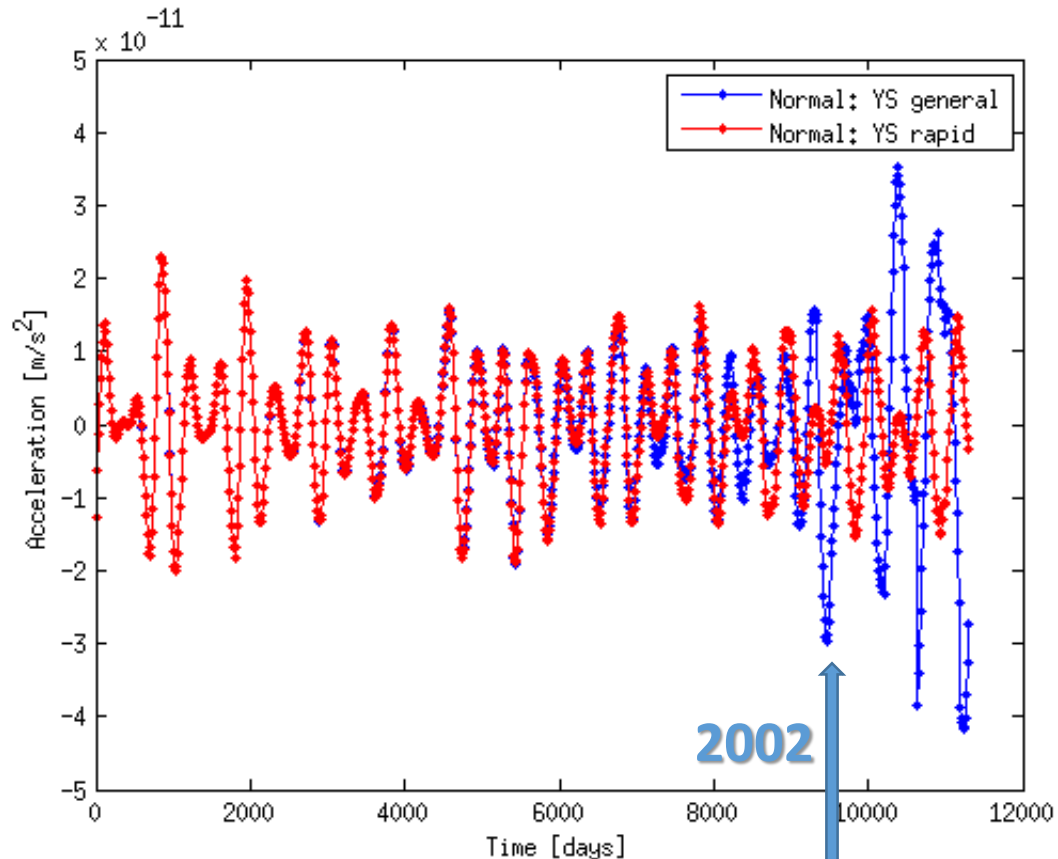


Thermal Thrust perturbations: the solar Yarkovsky–Schach effect

LARASE activities: comparison between the two models in the case of LAGEOS


Starting epoch, May 1976
Out-of-plane [W]

Argument of pericenter



Measurement of the relativistic precessions of the pericenter of LAGEOS II

Lucchesi, Peron, Phys. Rev. Lett., 105, 2010

PRL **105**, 231103 (2010)  Selected for a [Viewpoint](#) in *Physics*
PHYSICAL REVIEW LETTERS week ending
3 DECEMBER 2010



Accurate Measurement in the Field of the Earth of the General-Relativistic Precession of the LAGEOS II Pericenter and New Constraints on Non-Newtonian Gravity

David M. Lucchesi^{1,2} and Roberto Peron¹

¹*Istituto di Fisica dello Spazio Interplanetario, Istituto Nazionale di Astrofisica, IFSI/INAF,
Via del Fosso del Cavaliere 100, 00133 Roma, Italy*

²*Istituto di Scienza e Tecnologie dell'Informazione, Consiglio Nazionale delle Ricerche, ISTI/CNR,
Via G. Moruzzi 1, 56124 Pisa, Italy*

(Received 18 July 2010; published 29 November 2010)

Lucchesi, Peron, Phys. Rev. D, 89, 2014

PHYSICAL REVIEW D **89**, 082002 (2014)

LAGEOS II pericenter general relativistic precession (1993–2005): Error budget and constraints in gravitational physics

David M. Lucchesi^{*}

*Istituto di Astrofisica e Planetologia Spaziali, Istituto Nazionale di Astrofisica, (IAPS/INAF),
Via del Fosso del Cavaliere 100, 00133 Roma, Italy,
Istituto di Scienza e Tecnologie dell'Informazione, Consiglio Nazionale delle Ricerche, (ISTI/CNR),
Via G. Moruzzi 1, 56124 Pisa, Italy, and
Istituto Nazionale di Fisica Nucleare (INFN), Sezione di Pisa, Largo B. Pontecorvo 3, 56127 Pisa, Italy*

Roberto Peron

*Istituto di Astrofisica e Planetologia Spaziali, Istituto Nazionale di Astrofisica, (IAPS/INAF), Via del Fosso
del Cavaliere 100, 00133 Roma, Italy and
Istituto Nazionale di Fisica Nucleare (INFN), Sezione di Roma Tor Vergata,
Via della Ricerca Scientifica 1, 00133 Roma, Italy
(Received 16 April 2013; published 7 April 2014)*

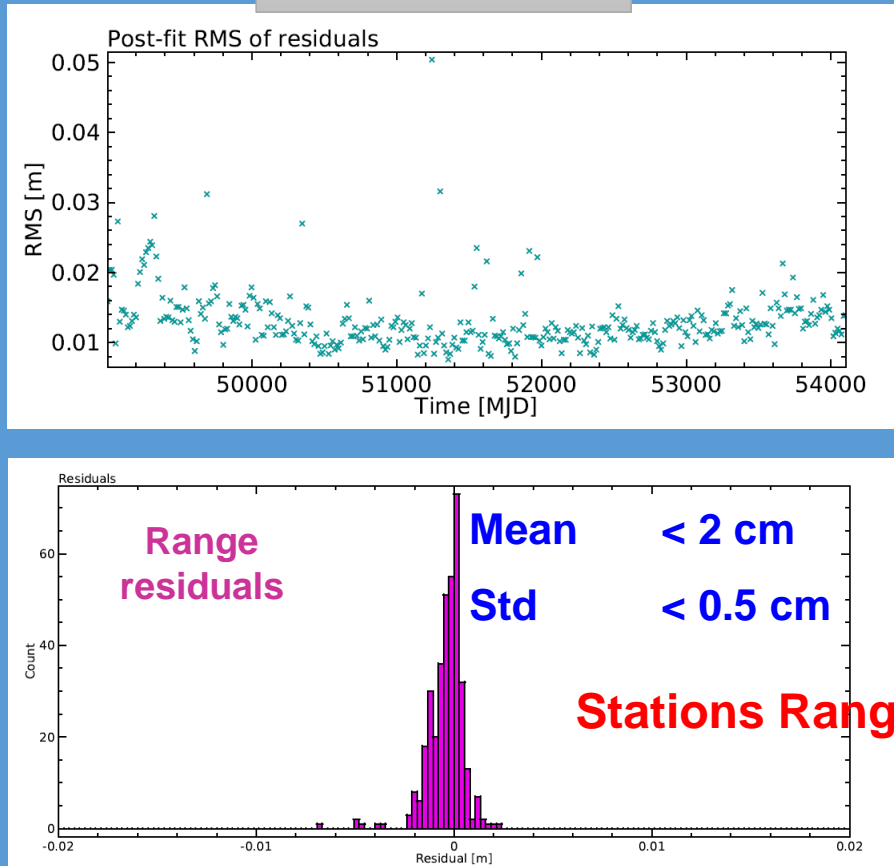
Measurement of LAGEOS II pericenter advance

**New measurement of LAGEOS II pericenter advance
and Error Budget**

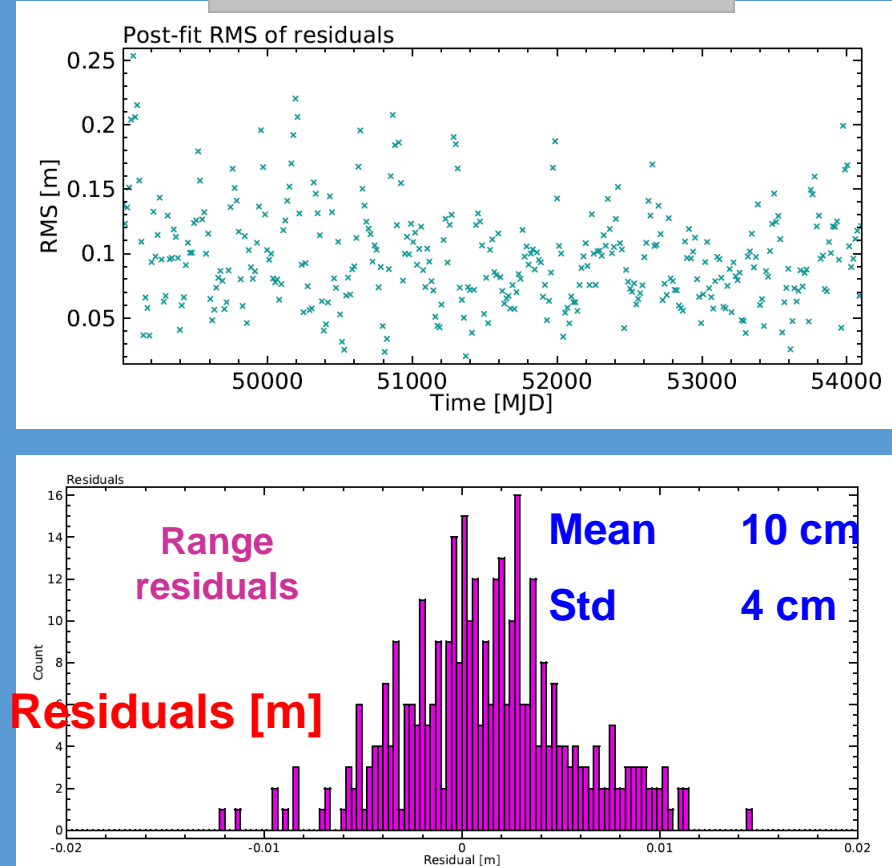
Measurement of the relativistic precessions of the pericenter of LAGEOS II

Data reduction accuracy: 13-yr analysis of the **LAGEOS II** orbit

Reference orbit



Orbit used in this work

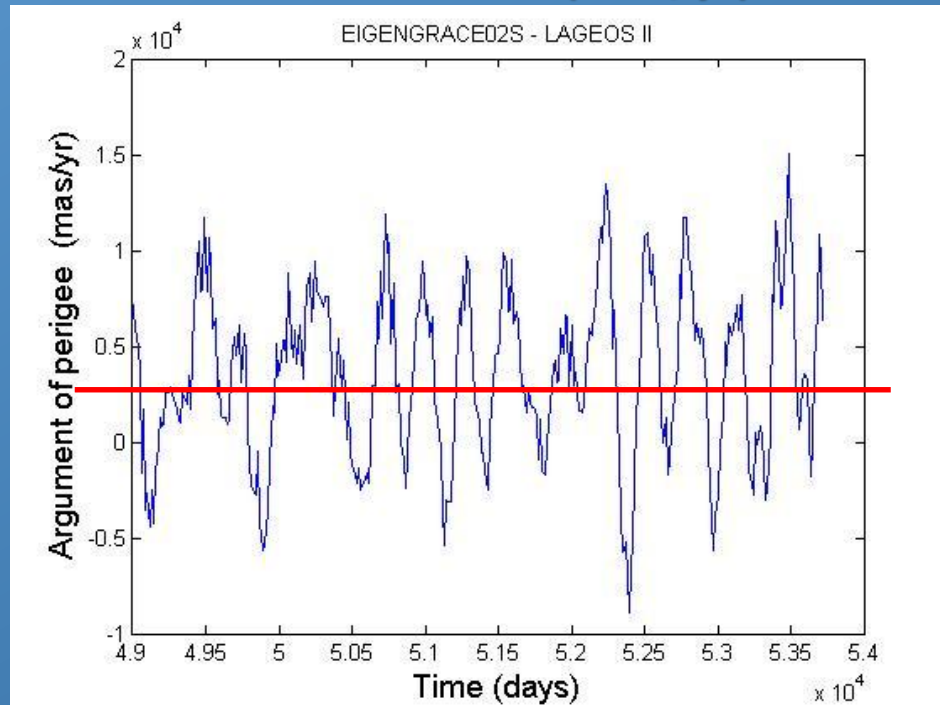


Measurement of the relativistic precessions of the pericenter of LAGEOS II

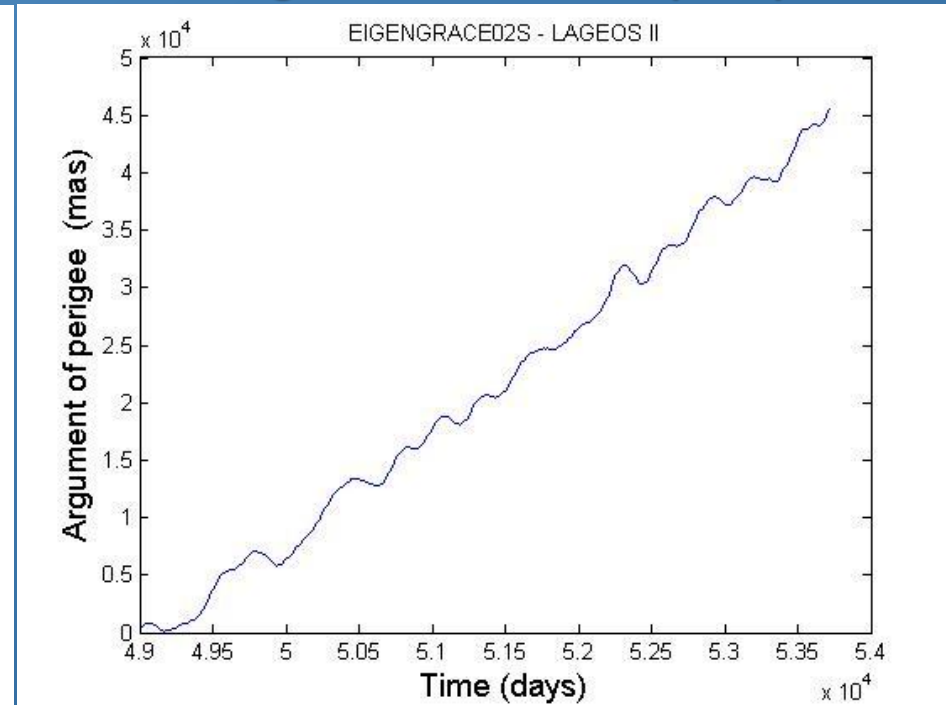
Data reduction accuracy: 13-yr analysis of the **LAGEOS II** orbit

Residuals of the argument of pericenter

Pericenter rate (mas/yr)



Integrated Pericenter (mas)

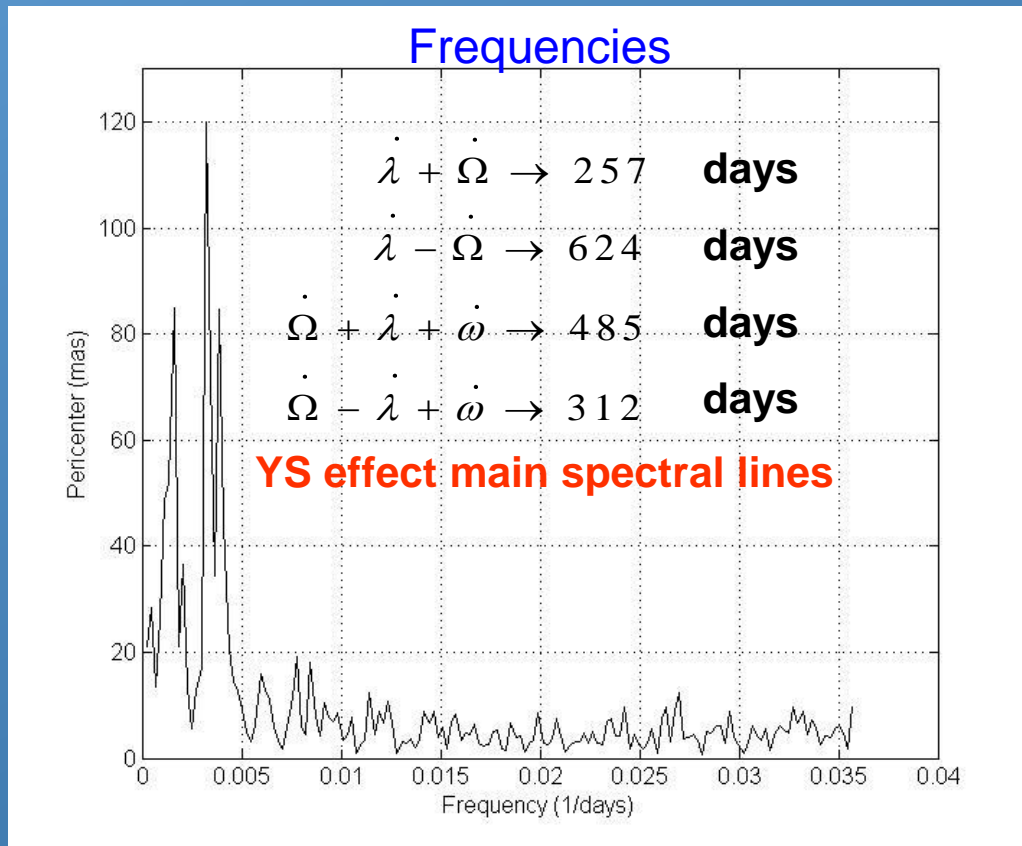


The perturbation due to the **YARKOVSKY–SCHACH** (YS) effect is clear from the residuals

Measurement of the relativistic precessions of the pericenter of LAGEOS II

Data reduction accuracy: 13-yr analysis of the **LAGEOS II** orbit

The FFT confirms the presence of the main spectral lines due to the YS effect



Fitting function for the pericenter:

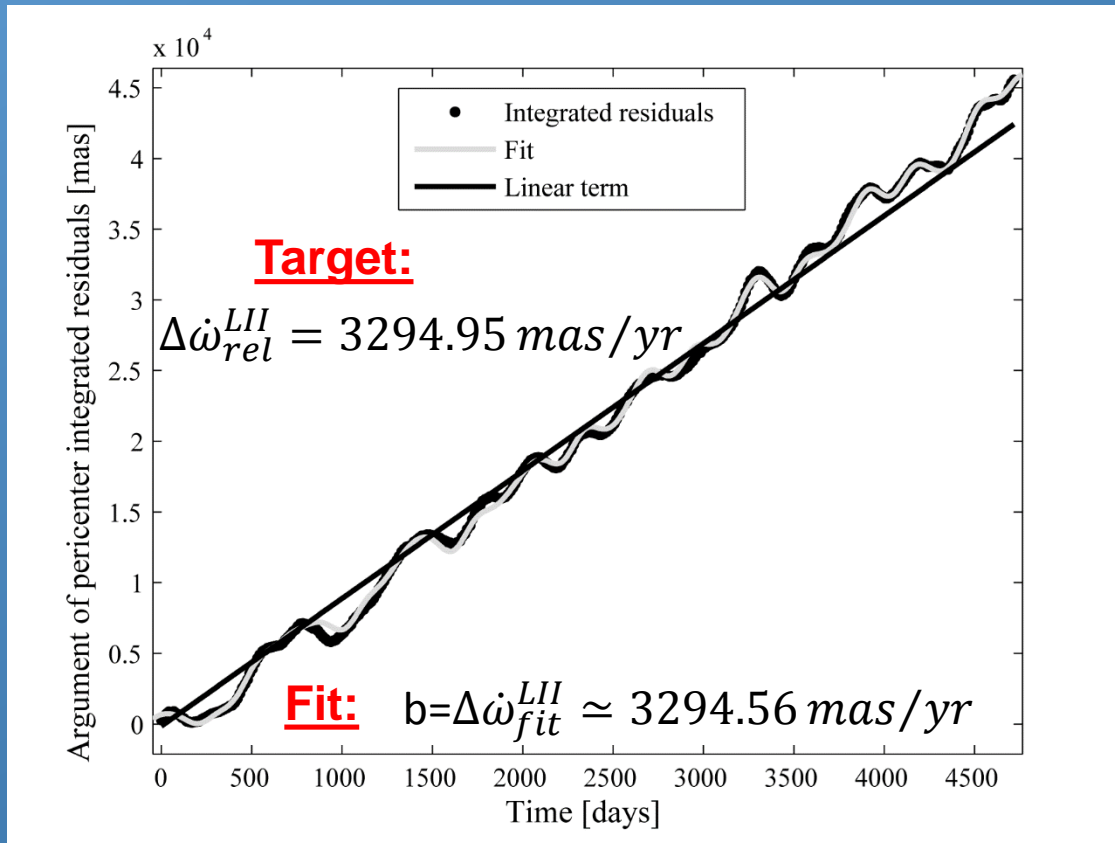
$$\Delta\omega^{FIT} = a + b \cdot t + c(t - t_0)^2 + \sum_{i=1}^n D_i \sin\left(\frac{2 \cdot \pi}{P_i} \cdot t + \Phi_i\right)$$

- with a , b , c , t_0 , D_i and Φ_i , free to vary from their nominal values (with no a priori constraint)
- and P_i fixed to their values from the FFT

Measurement of the relativistic precessions of the pericenter of LAGEOS II

Data reduction accuracy: 13-yr analysis of the **LAGEOS II** orbit

Fit to the pericenter residuals



Fitting function for the pericenter:

$$\Delta\omega^{FIT} = a + b \cdot t + c(t - t_0)^2 + \sum_{i=1}^n D_i \sin\left(\frac{2 \cdot \pi}{P_i} \cdot t + \Phi_i\right)$$

- We obtained $b \approx 3294.6 \text{ mas/yr}$, very close to the prediction of **GR**
- The discrepancy is just **0.01%**
- From a sensitivity analysis, with constraints on some of the parameters that enter into the least squares fit, we obtained an upper bound of **0.2%**

Measurement of the relativistic precessions of the pericenter of LAGEOS II

Final result for the relativistic precession of the **LAGEOS II** pericenter

Lucchesi & Peron, PRD, 89, 2014

For the result of our analysis of LAGEOS II pericenter general relativistic advance we assume the following conservative value:

$$\Delta \dot{\omega} = \Delta \dot{\omega}_{GP} + \Delta \dot{\omega}_{NGP} + \varepsilon \cdot \Delta \dot{\omega}_{GR}$$

$$\varepsilon = 1 - (0.12 \pm 2.10) \cdot 10^{-3} \pm 2.5 \cdot 10^{-2}$$

Best fit result 0.01%

Sensitivity analysis 0.2%

Systematic errors 2.5%

Where the ~ 2% error comes from an upper bound estimate of the systematic errors due to the gravitational and non-gravitational perturbations

Measurement of the relativistic precessions of the pericenter of LAGEOS II

DAVID M. LUCCHESI AND ROBERTO PERON

PHYSICAL REVIEW D **89**, 082002 (2014)

TABLE XVII. Error budget of the LAGEOS II pericenter general relativity shift. Top: summary of the errors from the data reduction and the *a posteriori* best fit (see Sections VI and VII). Middle: summary of the systematic errors from the gravitational perturbations (see Section VIII). Bottom: summary of the systematic errors from the nongravitational perturbations (see Section IX).

Statistical errors		
Residuals	Mean	Standard deviation
Range	9.67 cm	3.88 cm
Pericenter	4.57 mas	1.87 mas
Adjusted \mathcal{R}_a^2	0.998	
Reduced χ_ν^2 test	0.14	
$e_\omega^{\text{sta}} - 1 = (-0.12 \pm 2.10) \times 10^{-3}$		
Systematic errors: gravitational perturbations		
Error source	Error value (% $\Delta \dot{\omega}_{\text{II}}^{\text{rel}}$)	Total not correlated (% $\Delta \dot{\omega}_{\text{II}}^{\text{rel}}$)
Even zonal harmonics	2.45	
Odd zonal harmonics	4.10×10^{-2}	
Tides (solid + ocean)	2.48×10^{-2}	2.46
Secular trends ($\ell = \text{even}$)	3.30×10^{-2}	
Seasonal-like effects	0.24	
Systematic errors: nongravitational perturbations		
Error source	Error value (% $\Delta \dot{\omega}_{\text{II}}^{\text{rel}}$)	Total not correlated (% $\Delta \dot{\omega}_{\text{II}}^{\text{rel}}$)
Direct solar radiation	0.50	
Earth's albedo	0.39	
Thermal thrusts	0.09	0.64
Drag (neutral + charged)	negligible	
Total not correlated		2.54
$e_\omega^{\text{sys}} - 1 = \pm 2.54 \times 10^{-2}$		

Measurement of the relativistic precessions of the pericenter of LAGEOS II

Summary of the constraints in gravitational theories so far obtained

TABLE XVIII. Summary of the results obtained in the present work; together with the measurement error budget, the constraints on fundamental physics are listed and compared with the literature.

Parameter	Values and uncertainties (this study)	Uncertainties (literature)	Remarks
$\epsilon_\omega - 1$	$-1.2 \times 10^{-4} \pm 2.10 \times 10^{-3} \pm 2.54 \times 10^{-2}$...	Error budget of the perigee precession measurement in the field of the Earth
$\frac{ 2+2\gamma-\beta }{3} - 1$	$-1.2 \times 10^{-4} \pm 2.10 \times 10^{-3} \pm 2.54 \times 10^{-2}$	$\pm(1.0 \times 10^{-3}) \pm (2 \times 10^{-2})^a$	Constraint on the combination of PPN parameters
$ \alpha $	$\lesssim 0.5 \pm 8.0 \pm 101 \times 10^{-12}$	$\pm 1 \times 10^{-8b}$	Constraint on a possible (Yukawa-like) NLRI
$\mathcal{C}_{\oplus \text{LAGEOSII}}$	$\leq (0.003 \text{ km})^4 \pm (0.036 \text{ km})^4 \pm (0.092 \text{ km})^4$	$\pm(0.16 \text{ km})^{4c}; \pm(0.087 \text{ km})^{4d}$	Constraint on a possible NSGT
$ 2t_2 + t_3 $	$\lesssim 3.5 \times 10^{-4} \pm 6.2 \times 10^{-3} \pm 7.49 \times 10^{-2}$	3×10^{-3e}	Constraint on torsion

^aFrom the preliminary estimate of the systematic errors of [166] for the perihelion precession of Mercury.

^bFrom [167] with Lunar-LAGEOS GM measurements.

^cFrom [5] and based on a partial estimate for the systematic errors.

^dFrom [7] and based on the analysis of the systematic errors only.

^eFrom [168] with no estimate for the systematic errors.

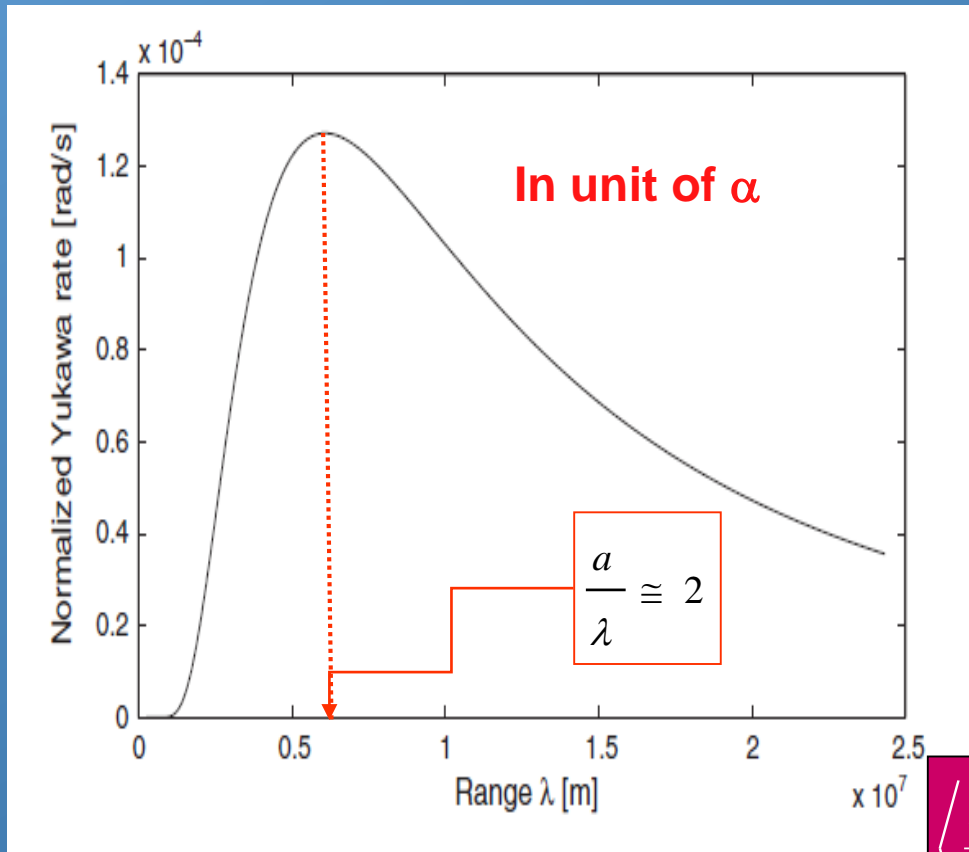
Measurement of the relativistic precessions of the pericenter of LAGEOS II

- Constraints on a long-range force: Yukawa-like interaction

Satellite pericenter shift (LAGEOS II)

$$\left\langle \dot{\omega} \right\rangle_{2\pi} = \frac{1}{2\pi} \int_0^{2\pi} -\frac{\sqrt{1-e^2}}{ena} (\Re \cos f) df$$

$$\Re = -\frac{G_{\infty} M_{\oplus}}{a^2} \left(\frac{a}{r}\right)^2 \alpha \left(1 + \frac{r}{\lambda}\right) e^{-\frac{r}{\lambda}}$$



Behavior of **LAGEOS II** pericenter rate perturbed by a Yukawa-like interaction as a function of the range λ

As we can see, the pericenter rate peaks for a value of the range λ of about 6081 km, very close to 1 Earth radius

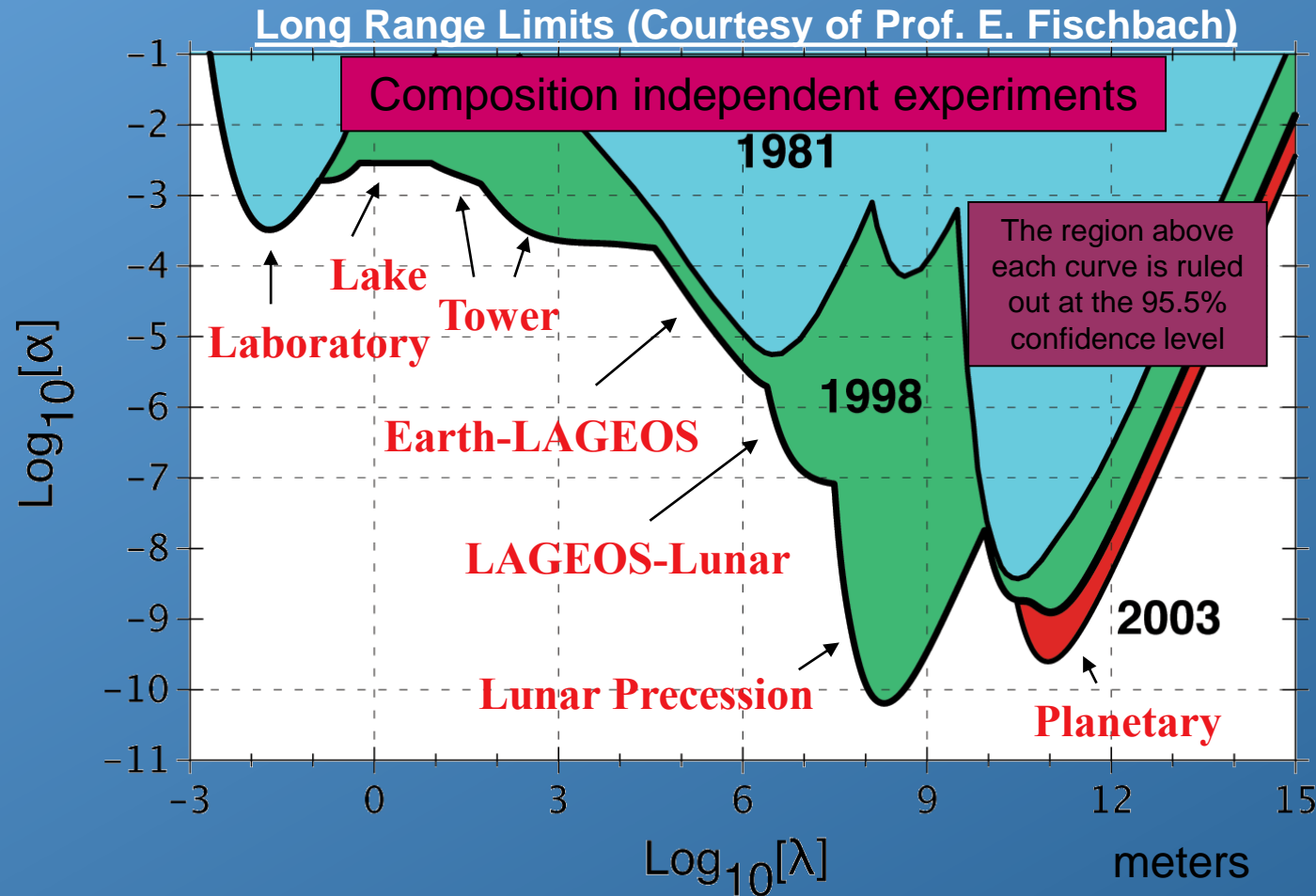
The peak value is about 1.27394×10^{-4} rad/s in unit of α

$$\left\langle \frac{d\omega}{dt} \right\rangle_{2\pi}^{Peak} \cong 1.27394 \cdot 10^{-4} \cdot \alpha \text{ rad/s}$$

$$\lambda \cong 6081 \text{ km} \approx 1 R_{\oplus}$$

Measurement of the relativistic precessions of the pericenter of LAGEOS II

- Constraints on a long-range force: Yukawa-like interaction



LAGEOS II
improvements

$$|\alpha| \cong |(0.5 \pm 8) \cdot 10^{-12} \pm 101 \cdot 10^{-12}|$$

$$|\alpha| \lesssim |1 \cdot 10^{-10}|$$

$$\lambda \cong 1R_{\oplus}$$

Previous limits with LAGEOS's:

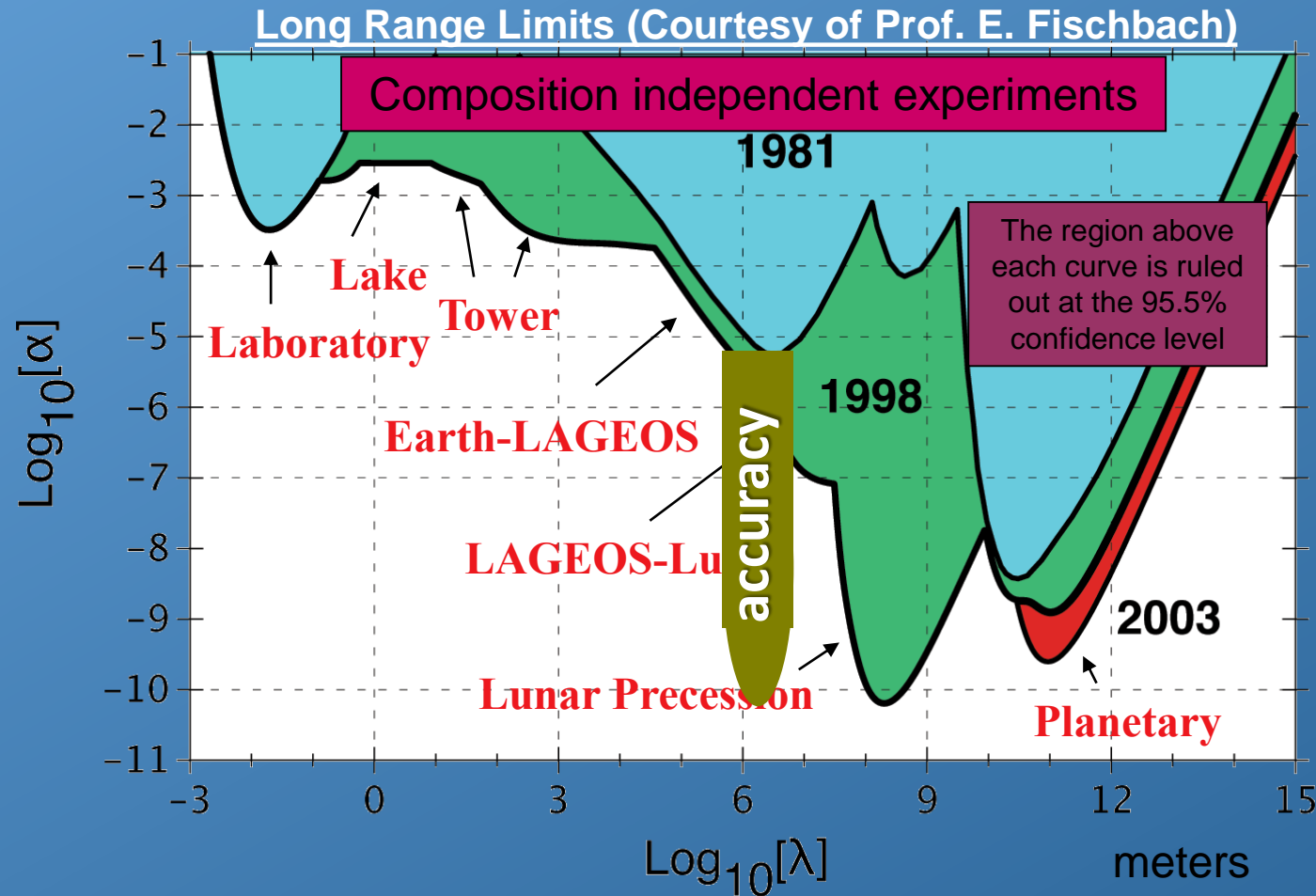
$$|\alpha| < 10^{-5} \div 10^{-8}$$

Li and Zhao, Int. Journ. Modern Phys D, 2005

Reference: Coy, Fischbach, Hellings, Standish, & Talmadge (2003)

Measurement of the relativistic precessions of the pericenter of LAGEOS II

- Constraints on a long-range force: Yukawa-like interaction



LAGEOS II
improvements

$$|\alpha| \cong |(0.5 \pm 8) \cdot 10^{-12} \pm 101 \cdot 10^{-12}|$$

$$|\alpha| \lesssim |1 \cdot 10^{-10}|$$

$$\lambda \cong 1R_{\oplus}$$

Previous limits with **LAGEOS's**:

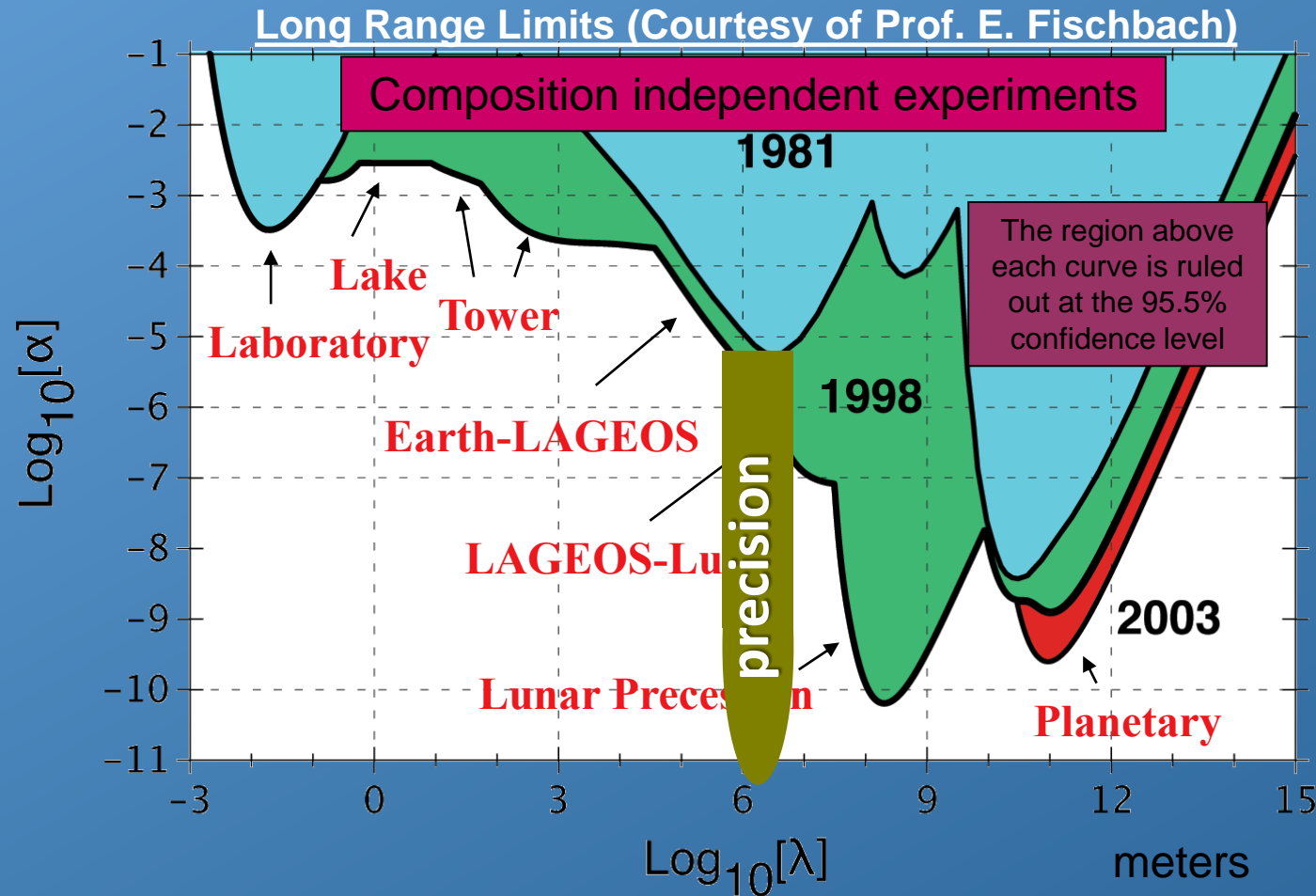
$$|\alpha| < 10^{-5} \div 10^{-8}$$

Li and Zhao, Int. Journ. Modern Phys D, 2005

Reference: Coy, Fischbach, Hellings, Standish, & Talmadge (2003)

Measurement of the relativistic precessions of the pericenter of LAGEOS II

- Constraints on a long-range force: Yukawa-like interaction



LAGEOS II
improvements

$$|\alpha| \cong |(0.5 \pm 8) \cdot 10^{-12} \pm 101 \cdot 10^{-12}|$$

$$|\alpha| \lesssim |8 \cdot 10^{-12}|$$

$$\lambda \cong 1R_{\oplus}$$

Previous limits with LAGEOS's:

$$|\alpha| < 10^{-5} \div 10^{-8}$$

Li and Zhao, Int. Journ. Modern Phys D, 2005

Reference: Coy, Fischbach, Hellings, Standish, & Talmadge (2003)